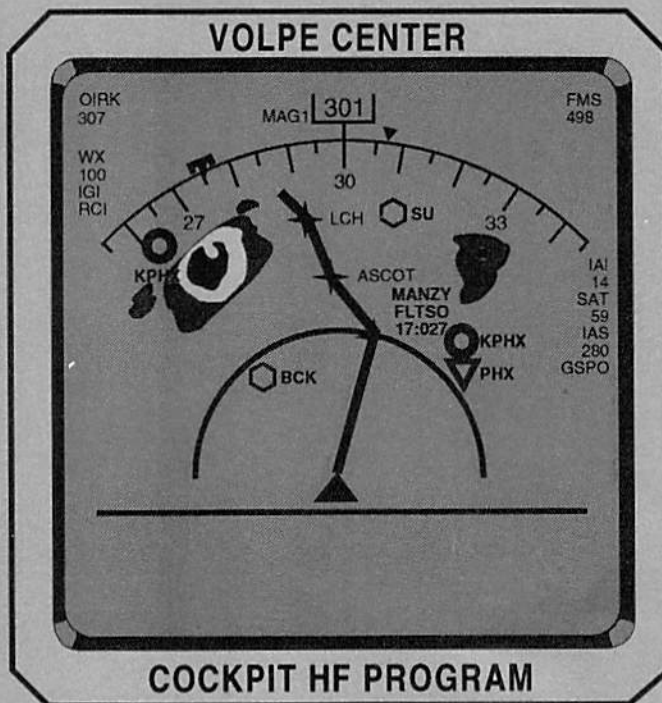




The Use of Analog Track Angle Error Display for Improving Simulated GPS Approach Performance

DOT/FAA/AR-95/104
DOT-VNTSC-FAA-95-29

Office of Aviation Research
Washington, DC 20591



U.S. Department of Transportation
Research and Special Programs Administration
John A. Volpe National Transportation Systems Center
Cambridge, MA 02142

Final Report
August 1995

This document is available to the public
through the National Technical Information
Service, Springfield, Virginia 22161



U.S. Department of Transportation
Federal Aviation Administration

NOTICE

This document is disseminated under the sponsorship of the Department of Transportation in the interest of information exchange. The United States Government assumes no liability for its contents or use thereof.

NOTICE

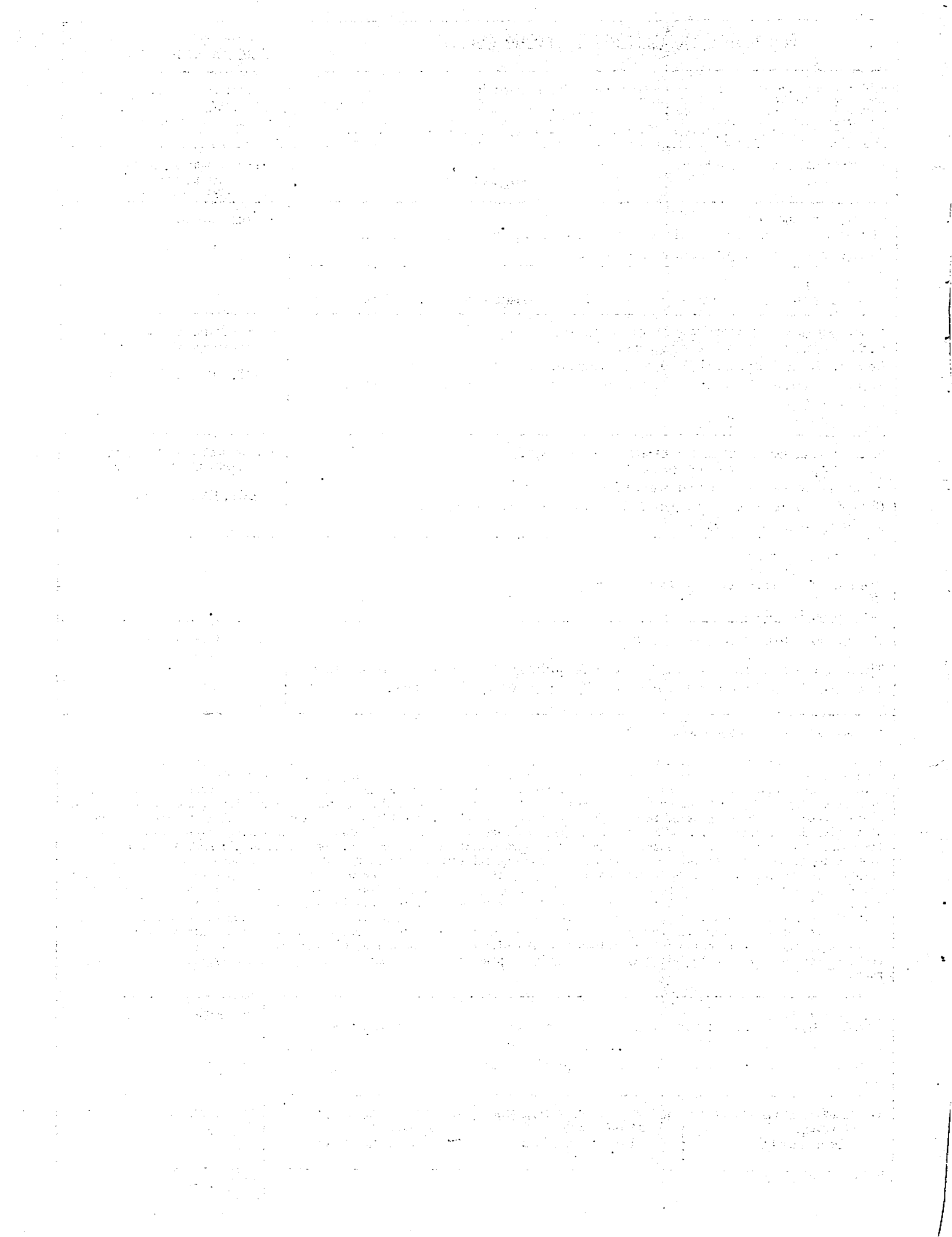
The United States Government does not endorse products or manufacturers. Trade or manufacturers' names appear herein solely because they are considered essential to the objective of this report.

REPORT DOCUMENTATION PAGE

Form Approved
OMB No. 0704-0188

Public reporting burden for this collection of information is estimated to average 1 hour per response, including the time for reviewing instructions, searching existing data sources, gathering and maintaining the data needed, and completing and reviewing the collection of information. Send comments regarding this burden estimate or any other aspect of this collection of information, including suggestions for reducing this burden, to Washington Headquarters Services, Directorate for Information Operations and Reports, 1215 Jefferson Davis Highway, Suite 1204, Arlington, VA 22202-4302, and to the Office of Management and Budget, Paperwork Reduction Project (0704-0188), Washington, DC 20503.

1. AGENCY USE ONLY (Leave blank)		2. REPORT DATE August 1995	3. REPORT TYPE AND DATES COVERED Final Report June 1994 - May 1995	
4. TITLE AND SUBTITLE The Use of Analog Track Angle Error Display for Improving Simulated GPS Approach Performance			5. FUNDING NUMBERS FA5E2/A5007	
6. AUTHOR(S) C.M. Oman*, M.S. Huntley, Jr., S.A. Rasmussen*, S.K. Robinson*				
7. PERFORMING ORGANIZATION NAME(S) AND ADDRESS(ES) U.S. Department of Transportation Research and Special Programs Administration John A. Volpe National Transportation Systems Center (VNTSC) Kendall Square Cambridge, MA 02142			8. PERFORMING ORGANIZATION REPORT NUMBER DOT-VNTSC-FAA-95-29	
9. SPONSORING/MONITORING AGENCY NAME(S) AND ADDRESS(ES) U.S. Department of Transportation Federal Aviation Administration Chief Scientific Technical Advisor for Human Factors Washington, DC 20591			10. SPONSORING/MONITORING AGENCY REPORT NUMBER DOT/FAA/AR-95/104	
11. SUPPLEMENTARY NOTES *Man Vehicle Laboratory Department of Aeronautics and Astronautics MIT Cambridge, MA 02142				
12a. DISTRIBUTION/AVAILABILITY STATEMENT This document is available to the public through the National Technical Information Service, Springfield, VA 22161			12b. DISTRIBUTION CODE	
13. ABSTRACT (Maximum 200 words) The effect of adding track angle error (TAE) information to general aviation aircraft cockpit displays used for GPS nonprecision instrument approaches was studied experimentally. Six pilots flew 120 approaches in a Frasca 242 light twin aircraft simulator using crosswind and turbulence. Twenty-five-mile-long approach geometries were used, with and without 45 degree dogleg turns on final approach. Performance and workload using three TAE display formats were compared against results with two control formats presenting cross track error (XTE) only. Pilots found that the TAE displays simplified determination of wind correction angle, and that they consistently chose to use analog rather than numeric TAE data. Statistically significant differences between display formats and between pilots were found. The largest average improvement in initial leg intercept and tracking performance resulted when the conventional "ten dot" XTE display was supplemented with a sliding pointer display of TAE, moving in the same direction as aircraft bank. A second TAE format, a sliding/rotating pointer integrated display, yielded the greatest improvement (35%) in the width of the short final approach flight technical error envelope, but pilots reported occasional problems interpreting this display. Both of these TAE formats improved final approach intercept and tracking performance after 45 degree turning maneuvers. The addition of TAE information to the receiver display helped pilots create outer loop lead, and yielded approach performance improvements comparable to relocating XTE information to an HSI within the pilot's primary scan. Bedford workload scores were not significantly influenced by display format, but were found to depend on approach geometry and phase.				
14. SUBJECT TERMS man/machine interfaces, displays, manual control, simulators, aircraft control, flight control, air traffic control, multiloop control, mental workload, global positioning systems, navigation systems			15. NUMBER OF PAGES 56	16. PRICE CODE
17. SECURITY CLASSIFICATION OF REPORT Unclassified	18. SECURITY CLASSIFICATION OF THIS PAGE Unclassified	19. SECURITY CLASSIFICATION OF ABSTRACT Unclassified	20. LIMITATION OF ABSTRACT	



PREFACE

This report presents the results of experimental studies on the effect of adding track angle error (TAE) information in analog form to general aviation aircraft cockpit displays used for global positioning system (GPS) non-precision instrument approaches. Pilots flew approaches in a light twin aircraft simulator using crosswind and turbulence. Twenty-five-mile-long approach geometries were used, with and without 45 degree dogleg turns on final approach. Performance and workload using three TAE display formats were compared against results with two control formats presenting cross track error (XTE) only.

This report is part of a continuing effort at the Volpe National Transportation Systems Center (Volpe Center) to develop human factors design guidelines for the electronic depiction of instrument approach procedures. Dr. M. Stephen Huntley, Jr. directed this research for the Volpe Center. This work was funded by the Federal Aviation Administration's (FAA's) Human Factors Program under the Office of Chief Scientific and Technical Advisor for Human Factors.

We thank G. Lyddane of the FAA, R. DiSario, D. Hannon, T. Carpenter-Smith, J. Bastow, F. Sheelen, J. Giurleo, and J. Turner, who all made important conceptual or technical contributions, and also our subjects. We also wish to thank M. Hendrickson, J. McBurney, and R. Frasca of Frasca International, Inc. The experimental protocol was approved by human use review committees at MIT and DOT/Volpe. Supported by MIT Center for Transportation Studies/DOT-Volpe Contract DTRS-57-92-C-0054 TTD#27A. Dr. Robinson was supported by a G.M. Low fellowship while on leave from NASA's Langley Research Center.

METRIC/ENGLISH CONVERSION FACTORS

ENGLISH TO METRIC

LENGTH (APPROXIMATE)

1 inch (in) = 2.5 centimeters (cm)
 1 foot (ft) = 30 centimeters (cm)
 1 yard (yd) = 0.9 meter (m)
 1 mile (mi) = 1.6 kilometers (km)

METRIC TO ENGLISH

LENGTH (APPROXIMATE)

1 millimeter (mm) = 0.04 inch (in)
 1 centimeter (cm) = 0.4 inch (in)
 1 meter (m) = 3.3 feet (ft)
 1 meter (m) = 1.1 yards (yd)
 1 kilometer (k) = 0.6 mile (mi)

AREA (APPROXIMATE)

1 square inch (sq in, in²) = 6.5 square centimeters (cm²)
 1 square foot (sq ft, ft²) = 0.09 square meter (m²)
 1 square yard (sq yd, yd²) = 0.8 square meter (m²)
 1 square mile (sq mi, mi²) = 2.6 square kilometers (km²)
 1 acre = 0.4 hectare (he) = 4,000 square meters (m²)

AREA (APPROXIMATE)

1 square centimeter (cm²) = 0.16 square inch (sq in, in²)
 1 square meter (m²) = 1.2 square yards (sq yd, yd²)
 1 square kilometer (km²) = 0.4 square mile (sq mi, mi²)
 10,000 square meters (m²) = 1 hectare (he) = 2.5 acres

MASS - WEIGHT (APPROXIMATE)

1 ounce (oz) = 28 grams (gm)
 1 pound (lb) = 0.45 kilogram (kg)
 1 short ton = 2,000 pounds (lb) = 0.9 tonne (t)

MASS - WEIGHT (APPROXIMATE)

1 gram (gm) = 0.036 ounce (oz)
 1 kilogram (kg) = 2.2 pounds (lb)
 1 tonne (t) = 1,000 kilograms (kg) = 1.1 short tons

VOLUME (APPROXIMATE)

1 teaspoon (tsp) = 5 milliliters (ml)
 1 tablespoon (tbsp) = 16 milliliters (ml)
 1 fluid ounce (fl oz) = 30 milliliters (ml)
 1 cup (c) = 0.24 liter (l)
 1 pint (pt) = 0.47 liter (l)
 1 quart (qt) = 0.96 liter (l)
 1 gallon (gal) = 3.8 liters (l)
 1 cubic foot (cu ft, ft³) = 0.03 cubic meter (m³)
 1 cubic yard (cu yd, yd³) = 0.76 cubic meter (m³)

VOLUME (APPROXIMATE)

1 milliliter (ml) = 0.03 fluid ounce (fl oz)
 1 liter (l) = 2.1 pints (pt)
 1 liter (l) = 1.06 quarts (qt)
 1 liter (l) = 0.26 gallon (gal)
 1 cubic meter (m³) = 36 cubic feet (cu ft, ft³)
 1 cubic meter (m³) = 1.3 cubic yards (cu yd, yd³)

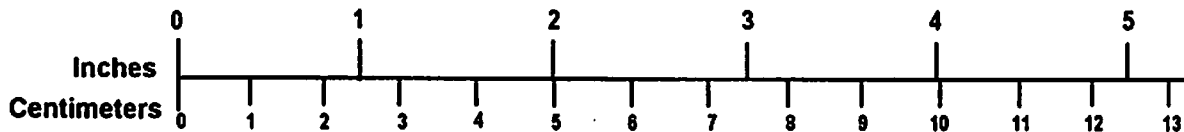
TEMPERATURE (EXACT)

$[(x-32)(5/9)]^{\circ}\text{F} = y^{\circ}\text{C}$

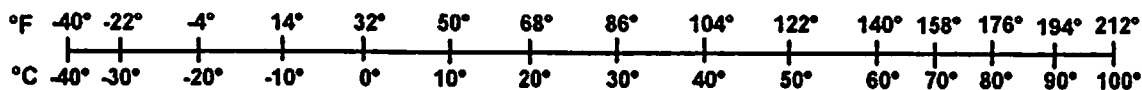
TEMPERATURE (EXACT)

$[(9/5)y + 32]^{\circ}\text{C} = x^{\circ}\text{F}$

QUICK INCH - CENTIMETER LENGTH CONVERSION



QUICK FAHRENHEIT - CELSIUS TEMPERATURE CONVERSION



For more exact and or other conversion factors, see NBS Miscellaneous Publication 286, Units of Weights and Measures.
 Price \$2.50 SD Catalog No. C13 10286

Updated 1/23/95

TABLE OF CONTENTS

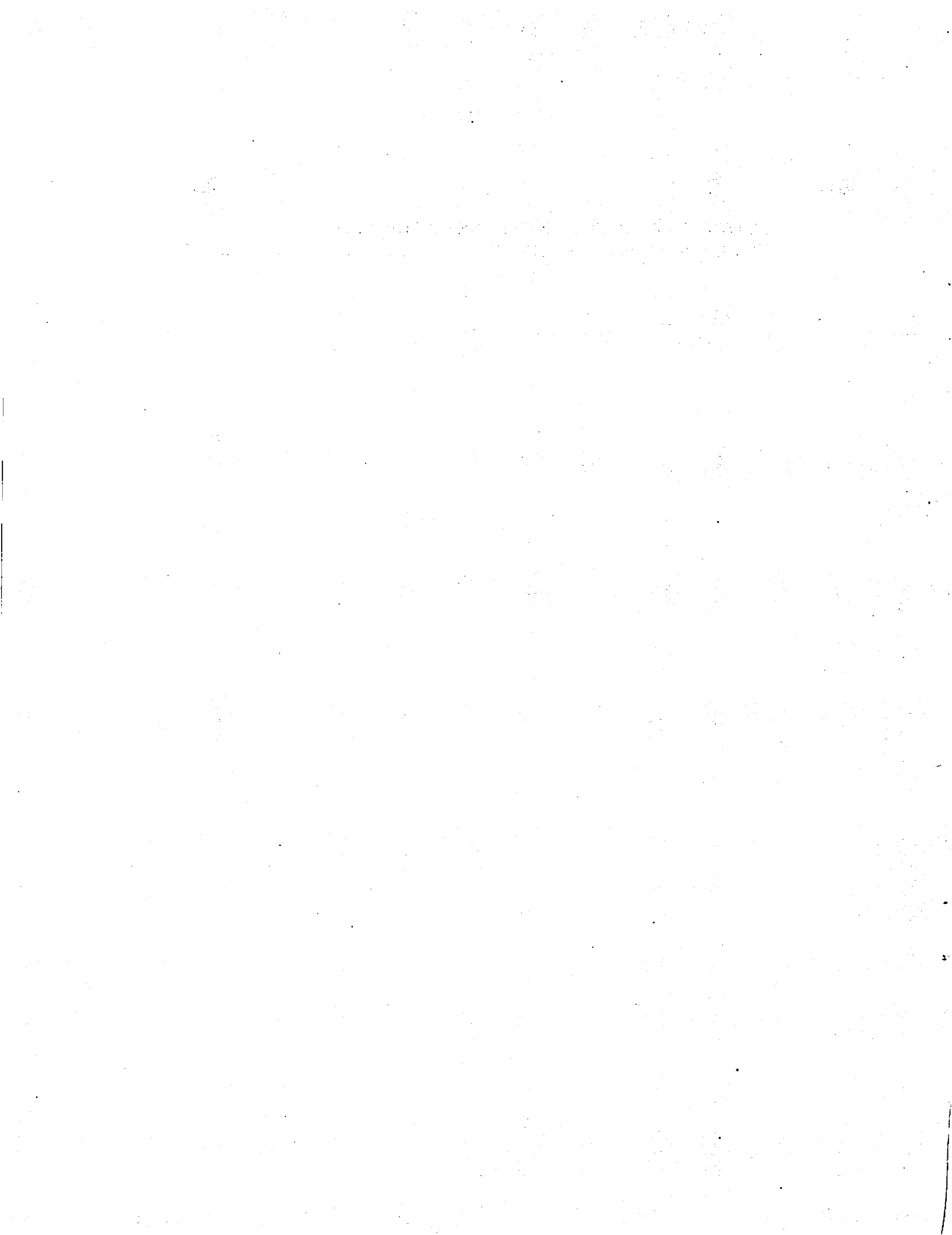
<u>Section</u>	<u>Page</u>
1. INTRODUCTION	1
2. METHODS	5
2.1 DISPLAYS.....	5
2.2 SUBJECTS, SESSIONS, AND EXPERIMENT DESIGN	6
2.3 AIRCRAFT, TURBULENCE, WIND SIMULATION, AND GPS APPROACH GEOMETRIES	7
2.4 WORKLOAD, DISPLAY PREFERENCE AND APPROACH PERFORMANCE METRICS.....	9
3. RESULTS	11
3.1 PILOT DISPLAY EVALUATIONS	11
3.2 PILOT DISPLAY PREFERENCES	12
3.3 INFLUENCES ON SUBJECTIVE WORKLOAD.....	13
3.4 DISPLAY EFFECTS ON GROUND TRACK, INTERCEPT, AND LEG TRACKING PERFORMANCE PARAMETERS.....	13
3.5 DISPLAY EFFECTS ON ESTIMATED 95% LIMITS OF CROSS TRACK ERROR.....	18
4. CONCLUSIONS.....	27
5. REFERENCES	29
APPENDIX A-1: FLIGHT SIMULATOR, COMPUTER NETWORK, TURBULENCE, AND WIND MODELS	31
APPENDIX A-2: APPROACH CHARTS	37

LIST OF FIGURES

<u>Figure</u>	<u>Page</u>
1.	(TOP): ANALOG XTE ON HORIZONTAL SITUATION INDICATOR CDI. (BOTTOM): ALPHANUMERIC DATA AS THEY MIGHT APPEAR ON NEARBY GPS RECEIVER DISPLAY..... 2
2.	ANALOG XTE CDI ON GPS RECEIVER DISPLAY..... 2
3.	THE DERIVATIVE OF CROSS TRACK ERROR (XTE) IS PROPORTIONAL TO TRACK ANGLE ERROR (TAE)..... 3
4.	THREE GPS TAE DISPLAY FORMATS STUDIED. TOP: TRIANGLE/SAME; MIDDLE: TRIANGLE/OPPOSITE; BOTTOM: TRACK VECTOR..... 6
5.	EXAMPLE OF THE NOS-STYLE GPS "T" APPROACH CHARTS USED. TOP: PLAN VIEW. BOTTOM: ELEVATION VIEW, MINIMA, AND FICTITIOUS AIRPORT DIAGRAM..... 8
6.	REORIENTED GROUND TRACK OVERLAYS FOR T AND "CROOKED T" APPROACHES, BY DISPLAY TYPE..... 14
7.	DEFINITIONS OF INTERCEPT PERFORMANCE MEASURES..... 15
8.	INTERCEPT ANGLE (DEGREES) VS. DISPLAY TYPE..... 16
9.	INTERCEPT DISTANCE FROM MAHF (NM) VS. DISPLAY TYPE. ... 16
10.	AVERAGE XTE (NM) FOR MILES 2-4 OF INITIAL APPROACH LEG VS. DISPLAY TYPE..... 17
11.	95% LIMITS OF XTE DISTRIBUTION FOR T APPROACHES ONLY. 19
12.	95% LIMITS OF XTE DISTRIBUTION FOR "CROOKED T" APPROACHES ONLY..... 21
13.	95% LIMITS OF XTE DISTRIBUTION FOR "CROOKED T" APPROACHES ONLY..... 23

LIST OF TABLES

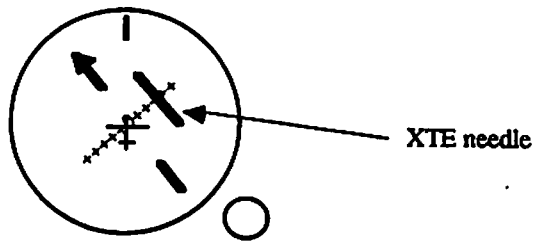
<u>Table</u>	<u>Page</u>
1. PILOT DISPLAY PREFERENCE RANKS BY DISPLAY, USING FOUR DIFFERENT SCALES	12



1. INTRODUCTION

Satellite-based navigation systems and a new generation of microprocessor-based cockpit avionics are revolutionizing air traffic control worldwide. In the United States, many transport and military aircraft are now equipped with global positioning system (GPS) based area navigation (RNAV) computers or flight management systems, which are used for supplementary en route and oceanic navigation. Research is underway to develop differential GPS systems with the horizontal and vertical accuracy and integrity needed for precision instrument approaches so that aging VOR and ILS nav aids can be phased out. Meanwhile, the horizontal accuracy of ordinary non-differential GPS receivers (100 m) is sufficiently good that the Federal Aviation Administration (FAA) encourages their use for less demanding non-precision approaches, employing conventional altimetry for descent. Pilots are now permitted to fly most existing non-precision approaches using GPS as the primary reference. The FAA has also begun to certify new approaches specifically designed for GPS-equipped aircraft. This initiative is particularly important for the general aviation (GA) community, since non-precision approaches to thousands of new airports will eventually be possible. Because GPS approach waypoints can be arbitrarily positioned, non-traditional approach geometries can be employed to improve obstacle clearance, or reduce noise and air traffic congestion. GPS RNAVs have flexible electronic displays, updateable databases, and many more operating modes than traditional VOR, DME, ILS, and ADF equipment. The new RNAVs can potentially make instrument flying both easier and safer, provided that the human factors aspects have been properly considered at the design stage.

GPS navigators for civil aircraft must meet minimum performance and display airworthiness standards established by the FAA (TSO C-129, and RTCA/DO-208). Approved units are now available from some manufacturers. In most GA aircraft, instruments are of the traditional "round dial" type, and panel space is limited. Hence, GPS navigators are typically stand-alone devices which occupy a radio or instrument slot. Only a small LCD or CRT display and a limited set of control buttons and knobs are practical. Since the GPS cross track error (XTE) information functionally replaces that from VOR, XTE is typically converted to an analog signal, and displayed on an existing VOR or ILS course deviation indicator (CDI), or Horizontal Situation Indicator (HSI) needle, as shown in Figure 1. Alternatively, a simulated CDI needle can be displayed on the navigation receiver itself (Figure 2). As with VOR-driven CDIs, the pilot always flies "toward" the needle to center it, but needle sensitivity is in linear, rather than angular units, and is scheduled: ± 5 nm full scale while en route, increasing to 1 mile during initial approach, to 0.3 miles 2 miles before final approach, and returning to 1 mile if a missed approach is flown.



NANCY	→	ANNIE	DTK 076
XTE	0.31		
DIST	1.2		
GS	124		

Figure 1. (Top) Analog XTE on Horizontal Situation Indicator CDI. (Bottom) Alphanumeric data as they might appear on nearby GPS receiver display

NANCY	→	ANNIE	DTK 076
XTE	0.31	[+ + + + 0 + + + +]	
DIST	1.2		
GS	124		

Figure 2. Analog XTE CDI on GPS Receiver Display

Maintaining an aircraft on course centerline using XTE information is a demanding manual control task. The pilot's stick position determines the third derivative of XTE. Human operators cannot stably control so-called "triple integral" dynamics by monitoring XTE alone. Pilots must monitor roll attitude and heading, and in a crosswind, use a cut-and-try technique to determine the proper wind correction angle. To avoid large oscillations across the course centerline, particularly during the critical stages of the final approach, pilots must partially base their control on the rate of change of XTE. In the parlance of manual control, this is called "outer loop lead." If XTE needle sensitivity is low, the rate of movement of the XTE needle is not easily perceived, especially since the pilot must frequently look to monitor other attitude, heading, airspeed and altitude instruments. On final approach, XTE needle sensitivity is deliberately increased to help the pilot see its movement and null small errors. However, when CDI sensitivity is high, the pilot must more frequently scan all instruments, reducing the time available to perform other tasks, and increasing workload. The pilot's ability to create outer loop lead is determined by instrument scanning delay (Clement et al., 1968). Any side task which delays instrument scan impairs tracking performance. In-flight studies have demonstrated a direct

relationship between CDI sensitivity and pilot workload, and an inverse relationship with XTE during non-precision approaches (Huntley et al., 1991) .

The capability of GPS RNAV systems to determine the direction of the aircraft's ground track with only a brief delay is potentially of importance for aircraft manual control. Since the desired heading is known, it is possible to compute "track angle error" (TAE), the difference between the desired track and the actual track. As shown in Figure 3, TAE is mathematically proportional to the rate of change of XTE, the important manual control variable. If TAE were displayed to the pilot, the pilot would not have to try to judge the rate of movement of the XTE needle. XTE could be less frequently scanned, and the pilot's performance might improve. There are several ways TAE information could be presented. One indirect method is to use TAE information to derive an inner loop attitude command. However, many GA aircraft lack the necessary flight director equipped attitude indicator. A second indirect method is to derive a TAE based "course to steer" — a heading flight director. However, this ideally requires an additional indicator on the primary heading display not available on existing instruments. Another option is to use TAE to estimate future XTE — a "predictor XTE" display. However, information on present XTE must also be presented, and specific information on the magnitude of the intercept angle may also be of interest to the pilot. A fourth alternative is simply to directly present TAE information on the GPS RNAV itself in analog form. It makes sense that if TAE were explicitly displayed, pilots might learn to take advantage of it.

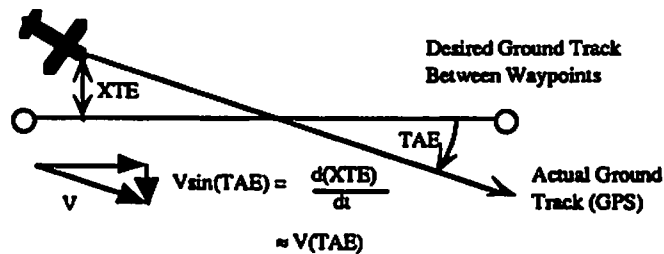


Figure 3. The derivative of Cross Track Error (XTE) is Proportional to Track Angle Error (TAE)

TSOed GPS RNAVs are required to have *at least* a numeric display of TAE. TSO C-129 suggests that "the use of non-numeric XTE data integrated with non-numeric TAE data into one display may provide the optimum of situation and control information for the best overall tracking performance." However, the TSO does not specify the graphical format of these displays, in part because pilot performance with analog TAE displays has never been formally investigated. The goal of this research was to begin this process via simulator experiments.

The purpose of this simulator research project was to see how pilots used explicit TAE information when it was presented numerically and also in analog form in several different formats. Which format do pilots favor, and why? To what extent does the addition of TAE information allow pilots to quantitatively improve their approach performance, or reduce their workload?

The first part of the document discusses the importance of maintaining accurate records of all transactions. It emphasizes that proper record-keeping is essential for the integrity of the financial system and for the ability to detect and prevent fraud. The text outlines the various methods used to collect and analyze data, including the use of statistical techniques and computerized systems. It also discusses the challenges of data collection and the need for standardized procedures to ensure consistency and reliability of the information.

The second part of the document focuses on the application of these principles in the context of a specific project or study. It describes the methodology used to gather data and the steps taken to ensure the accuracy and validity of the results. The text highlights the importance of transparency and the need to clearly document all aspects of the research process, from the initial data collection to the final analysis and reporting. It also discusses the potential limitations of the study and the need for further research to address these issues.

The final part of the document provides a summary of the key findings and conclusions. It reiterates the importance of accurate record-keeping and the need for standardized procedures to ensure the reliability of financial data. The text also discusses the implications of the findings for the broader field of financial research and the need for continued efforts to improve data collection and analysis methods. The document concludes with a call to action, urging researchers and practitioners to adopt the best practices outlined in the text to ensure the integrity and effectiveness of their work.

2. METHODS

2.1 DISPLAYS

The TAE GPS receiver display formats were evaluated in experiments performed using a modified, fixed base, light twin engine flight simulator (Frasca International, Inc. Urbana, IL, Model 242). A network of additional computers performed the GPS navigation calculations, created the displays and altitude dependent wind, and collected data. The display formats evaluated were:

1) Separate TAE and XTE sliding pointer displays (2 versions). This format,¹ shown in Figure 4 (top) added a TAE sliding pointer display beneath a conventional "fly to" XTE CDI. The TAE pointer was a triangle, located just beneath the XTE needle, and using the same "ten dot" (1.5-inch, 123-pixel-wide) scale. When the triangle was centered, TAE was zero. Full-scale TAE triangle deflection was set at ± 90 degrees, since this is the maximum useful course intercept angle. Which way should the TAE triangle move in response to a roll command? One alternative is to have the triangle move in the same direction as the stick roll command. This is easy to remember, and has the advantage that both the needle and the triangle appear on the same side of the display when converging with course. This version was therefore referred to as "Triangle/Same." However, a concern was that this makes the TAE triangle a "fly from" display. Since the XTE display above it is "fly to," this version apparently violates the well known human factors "command-response consistency" guideline. A second version of this format was also evaluated, where the sign of the triangle movement was reversed. This version was referred to as "Triangle/Opposite," and is shown in Figure 4 (middle).

2) A TAE/XTE sliding/rotating pointer integrated display. In this format, shown in Figure 4 (bottom), the needle was replaced with an (0.6-inch, 50-pixel-long) arrow, whose horizontal position was proportional to XTE and tilt angle was equal to TAE. This way, dimensional correspondence was preserved for the linear and angular variables. The sign of the arrow rotation was chosen so it always moved horizontally in direction of its tilt. In practice, the display resembled a "mail slot view" of a track up moving map display, where the arrow corresponded to the desired track, and the CDI scale to a downward-looking view of the aircraft's wings. If the pilot adopted this "inside out," aircraft centered frame of reference, interpretation of this display was very intuitive. This format was referred to as the "Track Vector" display.

To assess the value of explicit TAE information, these three displays were experimentally compared to an "XTE-only" receiver display, shown in Figure 2. All four formats required the pilot to frequently look over to the GPS receiver for XTE/TAE information, so a fifth format was also included, in which XTE was presented along with heading information on an HSI, and only

¹ Originally suggested by G. Lyddane, an FAA pilot, National Resource Specialist for Flight Management Systems, and an author of TSO C-129.

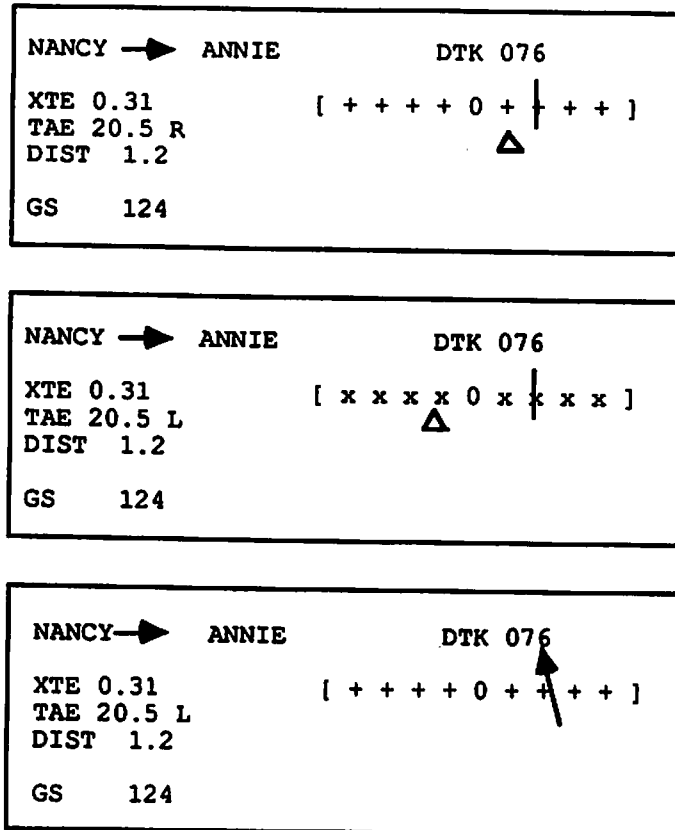


Figure 4. Three GPS TAE Display Formats Studied. Top: Triangle/Same; Middle: Triangle/Opposite; Bottom: Track Vector

alphanumeric information was presented on the receiver, as shown in Figure 1. The HSI was 70 cm from the pilot's eye, and 9.5 cm beneath the attitude indicator. The GPS receiver display was created on a high resolution LCD display, located 35 cm (27 deg) to the right of the HSI, in a 2 in. by 4 in. area subtending approximately 10 deg of horizontal visual angle. A consistent set of generic alphanumeric data was presented on all 5 displays: last and next waypoint, desired track (DTK), numeric XTE, groundspeed (GS), and distance (DIST) to waypoint. Numeric TAE was shown only on TAE displays. In all approaches, the pilot had to monitor DIST, and if a turn at the next waypoint was required, initiate a standard (3 deg/sec) turn at the appropriate point to intercept the next leg. Waypoints automatically sequenced when the aircraft crossed a line bisecting the angle between the inbound and outbound legs.

2.2 SUBJECTS , SESSIONS, AND EXPERIMENT DESIGN

Six multi-engine, instrument rated pilots were recruited locally. Total flight time averaged 1967 hr (range 750-3387 hr), and included an average of 73 hr (10-213 hr) actual instrument, 125 hr (30-370 hr) of simulated instrument, and 78 hr (4-240 hr) of time in various simulators. Multi-engine experience averaged 498 hr (22-1500 hr). They had flown an average of four (0-14) approaches and 26 hr (0-82 hr) in the past month, and an average of 6.3 hr (0-28 hr) in the week preceding the experiment.

Each pilot flew a total of 20 approaches, four with each of the five display formats, and two different types of approach geometries. Each approach required about 15 minutes, so the experiment was conducted in two ten-approach sessions on separate days. Pilots were given a written and oral briefing on the displays and the experiment procedures. Each day they flew the simulator and practiced with the displays until they felt familiar with them. They then flew 3-4 complete practice approaches with the different displays to asymptote practice effects, and then flew 10 test approaches. To minimize confusion between the two triangle formats, pilots flew with only one of the triangle formats each day. Half the subjects flew with the triangle/same first. The presentation order of triangle displays was thus blocked, but for the three other formats was randomized and balanced within sessions. The order was the same for all pilots.

2.3 AIRCRAFT, TURBULENCE, WIND SIMULATION, AND GPS APPROACH GEOMETRIES

Aircraft dynamics resembling a Piper Aztec were simulated via computer (Frasca 242 X4X-386 Flight System Model V1.11). To perturb the flight path, non-Gaussian, patchy turbulence (Jansen, 1981) was added about the three aircraft attitude axes. The disturbances qualitatively resembled moderate-severe turbulence, and required the pilot to closely monitor the attitude indicator to maintain control. Wind was always a 45 deg left or right head wind with respect to the final approach heading, but strength varied from 35 kt at 3100 ft above ground to 15 kt at the surface, using a power law atmospheric model. On many legs, up to 14 deg of heading correction was required. Pilots knew the wind direction varied, but were not told that only two relative wind directions were used.

Eight approach charts were employed. Each approach had a different final approach heading and required altitude, so that pilots could not memorize the numbers. Half the charts used a GPS "T" geometry, as shown in the Figure 5 example. The aircraft was initialized 0.5 nm upwind and abeam of the initial approach fix (IAF), located at one end of the top of the T. The pilot was required to intercept the initial approach leg, and fly 5 miles to an intermediate approach waypoint (IF) at the center of the "T," maintaining 3100 ft above ground level (AGL). At the IF, the pilot was instructed to turn 90 deg, and fly 5 miles to the final approach fix (FAF). A waypoint 2 miles before the FAF showed where XTE CDI sensitivity changed from ± 1 nm to ± 0.3 nm. The pilot was to lower the flaps and landing gear just before the FAF and, after passing it, fly 5 miles to the missed approach point (MAP) while descending to the 750 ft minimum descent altitude (MDA). At the MAP, the pilot was to retract gear and flaps, and climb back to 3100 ft AGL, flying to a first missed approach fix 5 miles directly ahead, make a second 90 degree, level turn, and then fly 5 more miles to a missed approach holding fix (MAHF). (Each chart had 2 or more IAFs, but the one used was always on the same side of the runway as the MAHF, so all turns were made in the same direction on any given run.) The turns permitted us to study performance while intercepting the subsequent leg. The initial, intermediate, and second miss legs were flown at constant altitude, and provided opportunities to measure tracking performance.

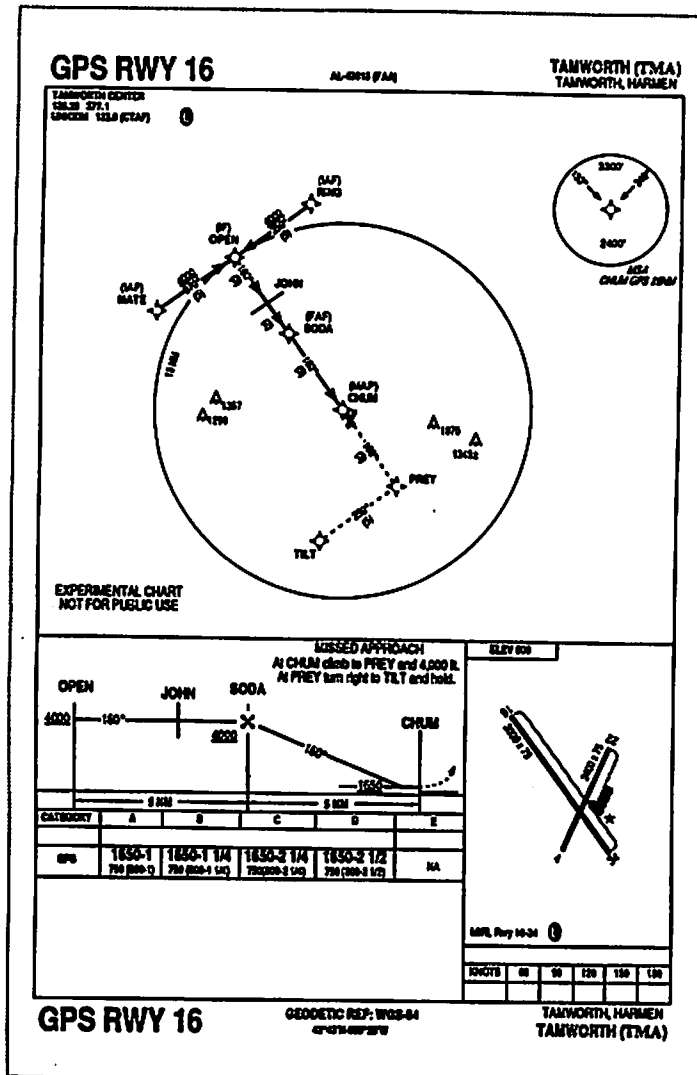


Figure 5. Example of the NOS-Style GPS "T" Approach Charts Used. Top: plan view. Bottom: elevation view, minima, and fictitious airport diagram

The remaining approaches used a "Crooked T" geometry² which required the pilot to also make a 45 deg turn while initiating descent at the FAF, and then fly a 2 mile descending dogleg before turning back to the runway heading. There was a minimum crossing altitude at the dogleg waypoint. Since these were descending turns made with 0.3 nm CDI sensitivity, the Crooked T approaches were expected to be much more difficult to fly.

During the approach and missed approach pilots were required to perform the usual checklist items, such as turning on and off fuel pumps and tuning the radio to a frequency found on the chart and announcing their position. All pilots were instructed to fly the approach and the missed

² The "T" approaches resembled an approved GPS approach at Oshkosh, WI. The "Crooked T" geometry was hypothetical, and chosen so that the pilot's ability to reintercept the final approach course after a maneuver could be evaluated.

approach at 120±10 kts, to fly as close to course centerline as possible, to maintain altitudes within 100 ft, but never to descend below the MDA.

2.4 WORKLOAD, DISPLAY PREFERENCE AND APPROACH PERFORMANCE METRICS

Immediately after each approach, pilots were asked to rate the overall workload on a 10 point modified Bedford workload scale, which emphasized spare attention (Roscoe and Ellis, 1990; Huntley et al., 1993). They were asked to describe any errors made, and then to rank in order the six legs of the approach from easiest to hardest. After the second test session, a questionnaire was administered which required the pilots to subjectively rank the five displays using several different display preference scales. These included ease of interpretation (EOI), effect on flight path control accuracy (FPA), and overall preference (OP). In addition, each pilot was asked to indicate relative preference between individual pairs of displays on a ± 7 point scale. The scores from these 10 pairs were summed using a tournament method, and ranked by display, to yield a second measure of overall preference based on direct “head-to-head” (HTH) comparisons.

Aircraft position and six performance parameters (XTE, TAE, altitude, airspeed, pitch and roll attitude) were sampled continuously at approximately 1 Hz by computer. Ground tracks from each of the 120 approaches were “normalized” (rotated to a common southerly final approach heading, east/west reversed where appropriate) and compared by display. The combined track records were used to retrospectively separate the approach into a series of 13 segments of varying lengths, chosen to isolate the various intercept, tracking, turning, descending and climbing phases of the approach. For purposes of comparison between display formats and pilots, the mean, standard deviation, and RMS values of all six performance parameters listed above were computed longitudinally along 13 different approach segments and analyzed using Systat v.5.2 (Systat, Inc., Evanston, IL). In addition, for each approach, XTE was sampled at half mile intervals along the desired track. XTE deviations on the same side of the desired track as the approach initiation point were taken as positive. At each successive location, samples were averaged by display format, and the mean and 95% limits of the XTE distribution were estimated for each slice along the desired track.³ Differences in tracking performance, as measured by the variance of XTE for different pairs of displays were assessed based on their F ratio.

Note that in this simulation, various GPS system errors — including the deliberate random error introduced by the US Department of Defense’s “Selective Availability” procedure — were not simulated. Hence, XTE provides a direct measure of “Flight Technical Error” (FTE), the discrepancy between the desired and actual position of the aircraft as displayed to the pilot.

³ The 95% limits of XTE were estimated based on a method originally proposed by Huntley (1993): The mean (M) and sample standard deviation (S) of XTE at each successive 0.5 nm location (“slice”) were computed, ensemble averaging across all approaches of the same type. Assuming XTE is normally distributed with a variance σ^2 , then (S/σ) is distributed as $(\chi^2/(n-1))^{0.5}$. If L is the tabulated $p=0.025$ value for $\chi^2/(n-1)$, then the 95% upper confidence limits of XTE can be estimated to be $M \pm 1.96 \cdot L^{0.5} \cdot S$.

1. The first part of the document discusses the importance of maintaining accurate records of all transactions and activities. It emphasizes that proper record-keeping is essential for transparency and accountability, particularly in the context of public administration and financial management.

2. The second part of the document outlines the various methods and tools used for data collection and analysis. It highlights the need for standardized procedures to ensure the reliability and validity of the information gathered.

3. The third part of the document focuses on the role of technology in modern data management. It discusses how digital tools and software can streamline processes, reduce errors, and provide real-time insights into organizational performance. It also touches upon the importance of data security and privacy in the digital age.

4. The fourth part of the document addresses the challenges faced in data management, such as data silos, inconsistent data quality, and limited access to information. It suggests strategies to overcome these challenges, including the implementation of data governance frameworks and the promotion of a data-driven culture within the organization.

5. The fifth part of the document concludes by summarizing the key findings and recommendations. It reiterates the importance of a systematic and integrated approach to data management, one that aligns with the organization's overall goals and objectives.

6. The final part of the document provides a brief overview of the future trends in data management, such as the increasing use of artificial intelligence and machine learning for data analysis and decision-making.

7. The document also includes a list of references and a bibliography, providing sources for further reading and research on the topics discussed.

8. Finally, the document includes a section for acknowledgments, recognizing the contributions of the individuals and organizations that supported the research and the development of the report.

3. RESULTS

3.1 PILOT DISPLAY EVALUATIONS

In debriefing evaluations, pilots noted that TAE displays had the following advantages over the XTE-only formats:

- a) When intercepting a new leg, pilots could choose an appropriate intercept TAE and then reduce it in several steps as they approached course centerline, to avoid overshooting.
- b) While tracking along a leg, an offset of the triangle or a tilt of the vector allowed pilots to detect and anticipate the magnitude and direction of slow changes in XTE.
- c) Pilots found that they could distinguish the "diverging" and "converging" XTE/TAE pointer configurations at a glance and react appropriately. For example, when the triangle/same pointers were on opposite sides of center, or when the track vector was tilted away from center, corrective action was immediately needed.
- d) When tracking, it was possible to immediately determine the crosswind correction angle without using trial and error. Pilots noted the heading when TAE equaled zero and many chose to set the heading indicator "bug" to this value, and simply made small left-right course corrections by flying one side of the bug. While training, pilots found it was possible to adopt a loop separation control strategy, using bank angle to control TAE and then TAE to control XTE, while largely ignoring heading. However, closed loop control of the TAE pointer required frequent scan of the TAE display. Most pilots found this difficult or inappropriate to do in turbulence, because the attitude indicators required so much attention, and instead relied on familiar attitude and heading control strategies, using TAE to command an appropriate heading.
- e) If the XTE indicator was off scale, an appropriate indication on the TAE pointer reassured the pilot that XTE would soon be on scale again.

The following TAE display deficiencies were noted:

- 1) Three pilots reported they occasionally had difficulty interpreting the track vector display. There appeared to be two reasons for this. The first was that the format resembled a conventional CDI, not a moving map display, and there was no explicit aircraft symbol in the center. Several pilots said they had "difficulty remembering which was the airplane and which was the track." The second was that the vector would suddenly "flip" by 90 deg during turns as the aircraft crossed the turn bisector. The pilot needed to mentally rotate the desired track reference frame in order to maintain the "inside out" map interpretation. Several pilots found they could not consistently do this.
- 2) Several pilots felt that small TAE offsets were more easily detected using either of the triangle displays than the vector display. In fact the graphical resolution of the track vector display was slightly better than the triangle displays (1.2 deg vs. 1.5 deg), but the track vector

pointer showed staircasing (aliasing) when it was nearly vertical, and there was no vertical reference mark.

It seems likely the track vector display could be improved by adding a fixed, central aircraft reference symbol and a surrounding outline box to promote the map interpretation, and a vertical reference mark to permit vernier judgments of tilt.

3.2 PILOT DISPLAY PREFERENCES

Post-session questionnaire data indicated a general preference for the triangle/same display over either of the other two TAE displays. At the same time, the rankings underscored the relative importance to the pilots of having XTE information in the primary instrument scan area, rather than alone on the GPS receiver. Results are shown in Table 1. A statistically significant effect of display was found for the HTH, FPA, and EOI scale rank scores from the individual subjects (Friedman rank ANOVAs, $p < 0.04$). For the OP scale results, the display effect was at the $p < 0.06$ level.

Table 1. Pilot Display Preference Ranks by Display, Using Four Different Scales (see text). Rank = 1 is best.

Display Format	Display Preference Scales			
	OP	HTH	FPA	EOI
Δ/Same	2	2	1	2
Δ/Opposite	3	4	2	5
Vector	4	3	4	3
HSI	1	1	3	1
XTE only	5	5	5	4

On the Overall Preference (OP) and Head-To-Head (HTH) comparison scales, pilots consistently preferred the HSI display over the “triangle/same” TAE display. However, in terms of summed rank scores, the margin was slight. When asked to make head-to-head comparisons, half the pilots preferred the triangle/same display, two preferred the HSI display, and one judged it a tie. Directly comparing the “triangle/same” and “triangle/opposite” versions, four pilots preferred the former, and only one pilot preferred the latter. All pilots always ranked one or more of the TAE display formats above the XTE-only on both scales, so the consensus was clear that TAE information was subjectively useful.

For accurate flight path control, pilots preferred the triangle/same display, though the three subjects (1, 4, and 5) who actually tracked most consistently ranked the HSI first in this respect. Four of the five pilots said the HSI was the easiest of the displays to interpret, though three of the four cited long-standing training and experience with the HSI format as one reason for this preference.

Four of the six pilots said they never referred to the numeric TAE information at all, since it was not obvious how to interpret the L/R TAE indication, and because the analog TAE pointer was available.

3.3 INFLUENCES ON SUBJECTIVE WORKLOAD

Average Bedford subjective workload was 3.5 out of 10 on T approaches, and increased to 4.5 on Crooked T. Subject 2 had the highest average workload (6.2) and Subject 1 the lowest (3.0). ANOVA of modified Bedford Workload scores revealed significant effects between subjects ($F(5,108)=29$; $p<0.0001$), and T and Crooked T approach types ($F(1,108)=28.4$; $p<0.0001$). The least mean square workload scores by display type were estimated as: triangle/same=3.8; triangle/opposite=3.9; track vector=4.0, HSI=3.9; XTE only=4.5. However, adding display to the ANOVA did not produce a significant effect. No trends were found by sequential approach or session number, suggesting training had asymptoted practice effects. Ranking workload scores within subjects did not reveal a display dependent effect. It was concluded that although the workload metric was demonstrably sensitive to approach geometry, display effects, if they exist, must be small compared to geometry and inter-subject effects.

The pilots ranked the approach legs in order of decreasing difficulty: 1) long/dogleg final, 2) short final, 3) intermediate leg, 4) first miss, 5) initial leg, and 6) second miss leg. Ranking was identical for both approach geometries, and the concordance of workload rankings within geometries was statistically significant (Friedman ANOVA, $df=5$; $p<0.0001$).

3.4 DISPLAY EFFECTS ON GROUND TRACK, INTERCEPT, AND LEG TRACKING PERFORMANCE PARAMETERS

The reoriented aircraft ground tracks are shown superimposed in Figure 6, staggered by the five display types. The Crooked T tracks can be distinguished by the dogleg after the FAF. Several approaches where pilots made gross errors are apparent, particularly for the XTE-only display (upper right). The frequency of such errors was noted to be less with the HSI and triangle/same displays (left and third from left).

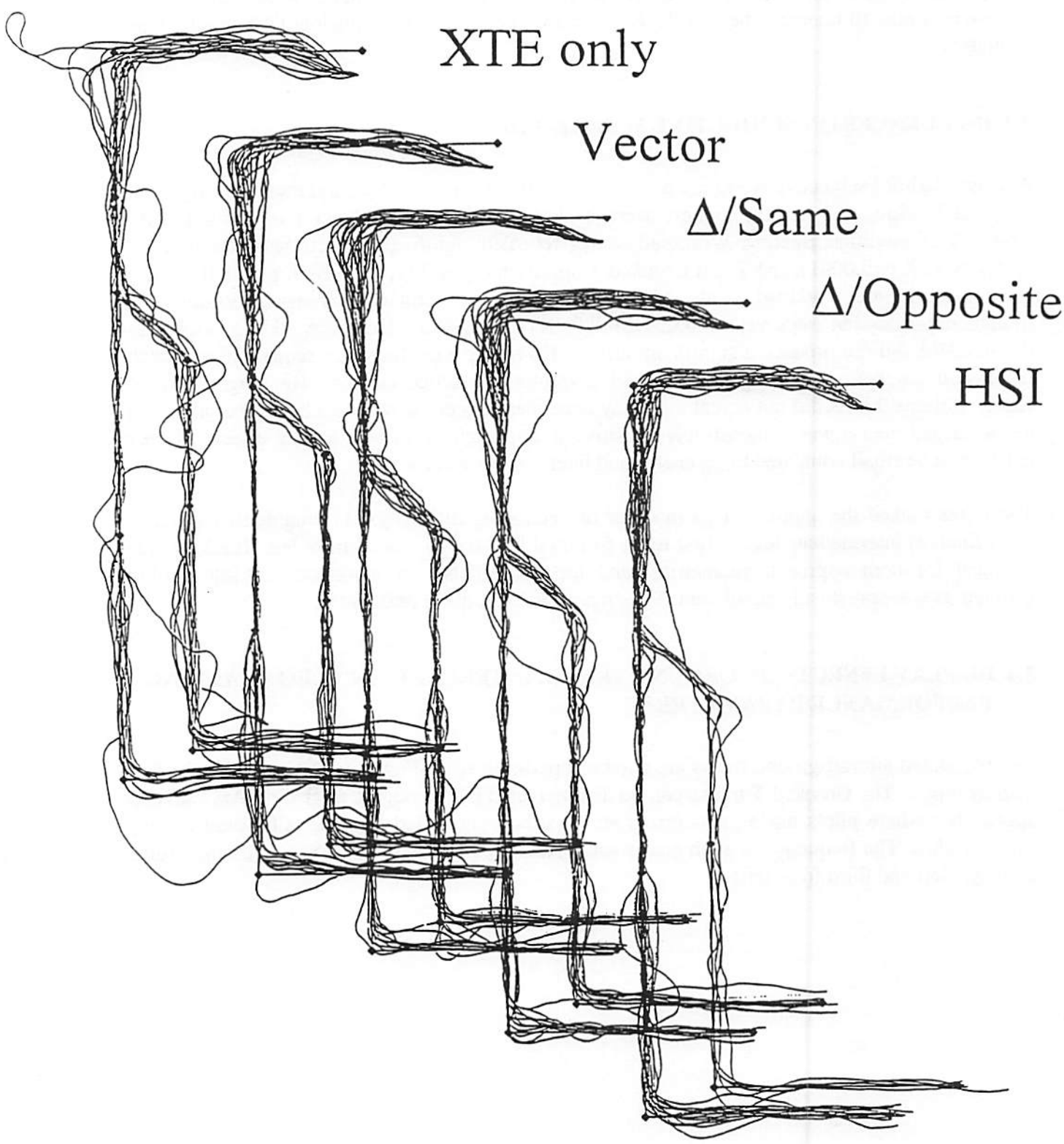


Figure 6. Reoriented Ground Track Overlays for T and "Crooked T" Approaches, by Display Type

When the simulation began, with the aircraft positioned a half mile upwind of the IAF, the pilot's first task was to intercept the initial approach leg. Use of TAE displays resulted in different intercept performance, probably because pilots were less aware of the crosswind component (always from the right in Figure 6), which inherently tended to blow the aircraft toward the desired track, and some failed to compensate for it. Two measures of intercept performance were assessed, as shown in Figure 7: 1) "Intercept Angle," the absolute value of TAE when XTE equaled 0.3 nm, and 2) "Intercept Distance," the distance where the aircraft first crossed within 0.05 nm of the initial approach centerline. As shown in Figures 8 and 9, Intercept Angle and Intercept Distance were consistently steeper and shorter, respectively, for approaches made with the non-TAE displays. The average increase in intercept angle with non-TAE formats approximated the drift angle to be expected (12 deg) for pilots unaware of the crosswind. ANOVA of intercept angle data showed significant effects by display ($F(4,85) = 24.1, p < 0.0001$), subject ($F(5,85) = 4.6, p < 0.001$), and subject by display ($F(20,85) = 1.7, p < 0.04$). Similarly, an intercept distance ANOVA revealed significant effects by display ($F(4,85) = 23.9, p < 0.0001$), subject ($F(5,85) = 4.6, p < 0.001$) and subject by display ($F(20,85) = 2.1, p < 0.007$). The significant subject by display interaction effects indicate that some subjects used the TAE information differently than others. Contrasts comparing TAE and non-TAE intercept angle and distance results by display were both significant ($p < 0.0001$).

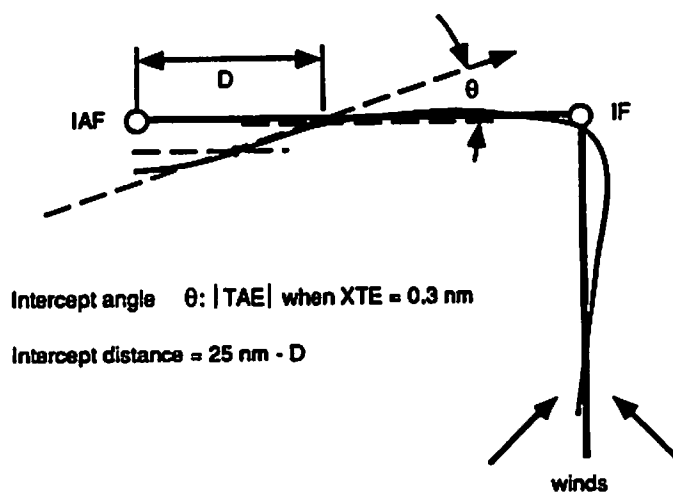


Figure 7. Definitions of Intercept Performance Measures

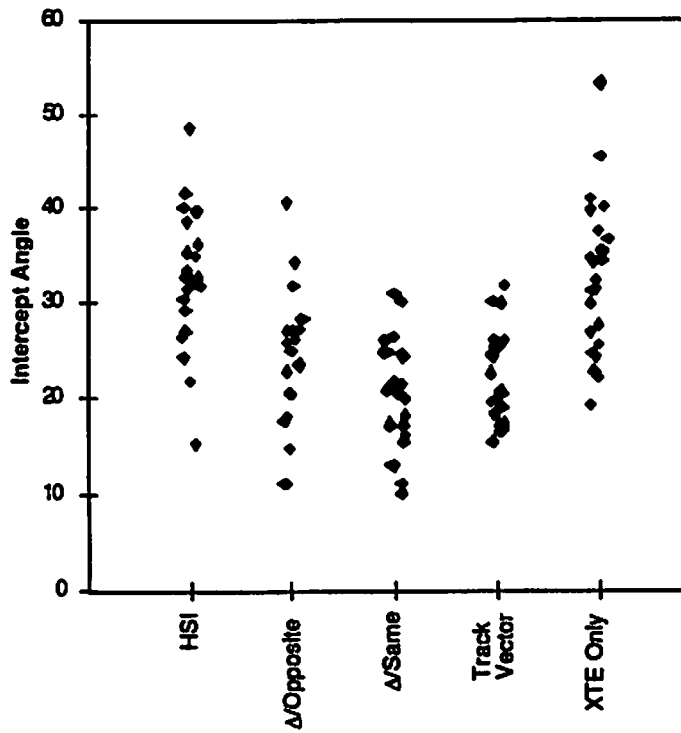


Figure 8. Intercept Angle (Degrees) vs. Display Type

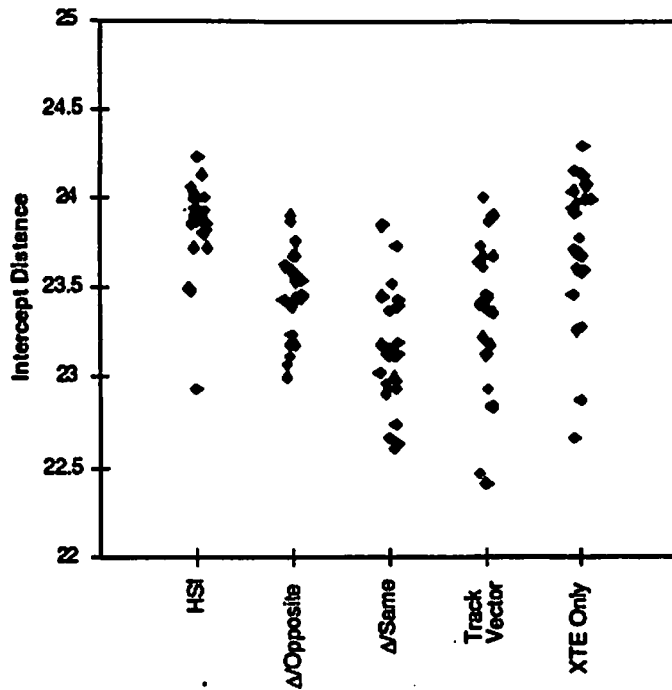


Figure 9. Intercept Distance from MAHF (nm) vs. Display Type

Once established on the initial leg, pilots flying with the triangle/same and vector displays had smaller downwind biases, as shown in Figure 10. The difference in average tracking bias was significant by display ($F(4,90) = 7.8, p < .001$) and subject. ($F(5,90) = 6.4; p < .001$). The subject by display interaction was not significant.

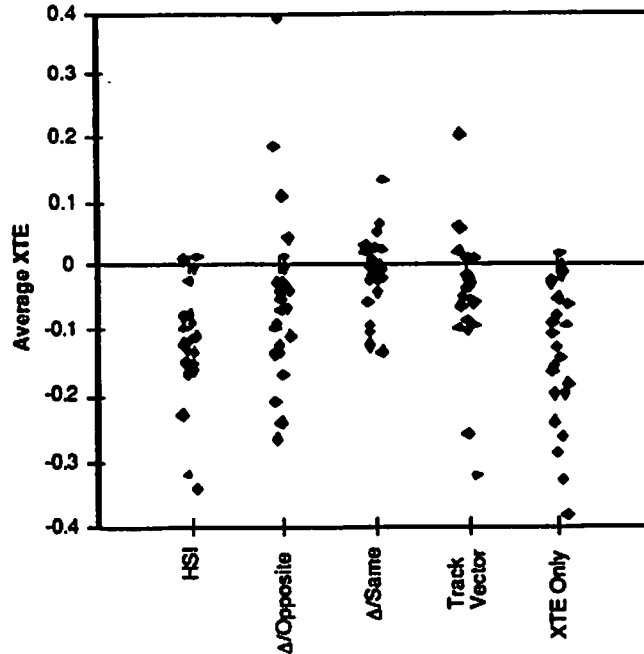


Figure 10. Average XTE (nm) for Miles 2-4 of Initial Approach Leg vs. Display Type

Considering the XTE and TAE data from the tracking portions of the initial, intermediate, and second missed approach legs (i.e., combining data obtained from miles 23-21, 19-17, and 4.5-1 from the MAHF), ANOVA demonstrated significant effects of display ($F(4,329) = 2.7, p < 0.03$) and subject ($F(5,329) = 14.8, p < 0.0001$) for the standard deviation of XTE and also the standard deviation of TAE (display: $F(4, 168) = 4.9, p < 0.001$; subject: $F(5, 168) = 11, p < 0.0001$). This was consistent with the hypothesis that pilots in fact were controlling TAE. The subject by display interaction term was also significant, indicating that certain subjects made better use of the TAE information than others. The HSI or triangle/same displays generally ranked best in terms of performance, followed by the track vector display. Average display effects were smaller than subject effects. The standard deviation of XTE was consistently lower on the final approach leg, as the aircraft approached the MAP.

Inter-subject differences in XTE and TAE tracking performance correlated with inner loop attitude control for the corresponding segments. Two subjects (2 and 6) consistently showed larger values of standard deviation of pitch and roll attitude, airspeed, and altitude, suggesting that their effective attitude instrument scanning delay was longer. There was no clear effect of display format in the longitudinal axis on pitch, airspeed, and altitude, but for the lateral/directional axis, ANOVA revealed a significant effect of both subject ($F(5,449) = 59, p < .0001$) and display ($F(4,449) = 3.9, p < .004$) on the variation in roll attitude. No correlation of segment performance with pilot recent or total experience was found, except for pilot 2, whose recent instrument time was only in helicopters.

3.5 DISPLAY EFFECTS ON ESTIMATED 95% LIMITS OF CROSS TRACK ERROR

To assess the effects of display format on flight technical error, the estimated 95% limits of the XTE distribution were plotted⁴ for the T approaches (Figure 11), the Crooked T approaches (Figure 12) and all approaches combined (Figure 13). Each of the three figures has ten panels, which compare the width of the XTE envelopes pairwise by display. In each panel, the shaded regions depict the 95% limits (in feet) estimated using the sample variance of the normalized track data for each slice. As shown in the key, the ordinate is distance along the desired track measured from the MAHF. Only data between 23 miles (typical initial intercept) through 10 miles (MAP) are shown. Diamonds on the ordinate denote waypoints, as indicated in the key. Circles and crosses denote slices where an F ratio test comparing the XTE sample variance for the two displays showed a significant difference. Note that the upper confidence limits for the XTE variance depend on the number of approaches.

The analysis of the XTE slice data revealed significant differences between displays during initial, intermediate, and final approach:

a) On the initial approach leg, F ratio tests showed the triangle/same display XTE envelope was significantly narrower than all other displays (c.f. Figure 13b, e, g, and i). Also, the centers of the initial approach envelopes for the HSI and XTE only formats were clearly displaced downwind, as indicated by negative envelope mid values in Figures 13d for 23-21 miles, as compared to all three TAE based displays (Figures 13a-c, h, i, and j). The latter finding reflects the significant difference in tracking bias effect described earlier (Figure 10).

b) During and immediately after the 90 deg turn at the IF, pilots using the HSI had significantly narrower XTE envelopes than with any of the other displays (Figures 13a-d), by F ratio test. As compared to the other displays, the track vector display envelope remained relatively wide between the IF and the sensitivity changeover waypoint (Figures 11 and 12c, e, f, and h). Thereafter, however, XTE rapidly converged.

c) On T geometry final approaches, the track vector display envelope was narrower than for any of the other displays (Figures 11 c, e, f, and h), significantly so on short final, one mile from the MAP. The differences between displays disappeared at the MAP itself, perhaps because by then the pilots had shifted their attention to missed approach activities. Average 95% XTE envelope width during the last three miles of final approach provides a useful metric for approach performance comparisons. Average envelope widths were: HSI: 0.17 nm, triangle/opposite: 0.22 nm, triangle/same: 0.21 nm, track vector: 0.15 nm, and XTE only: 0.23 nm. Comparing the track vector result with that of XTE only, deletion of TAE vector information from the receiver display resulted in a 53% increase in the average envelope width.

⁴ Two approaches with large, outlier XTE values due to pilot disorientation were omitted from the analysis.

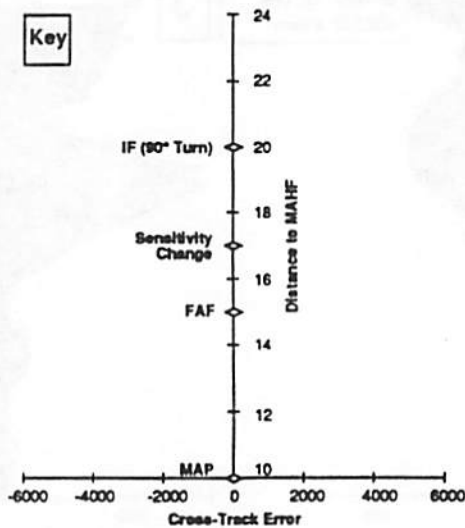
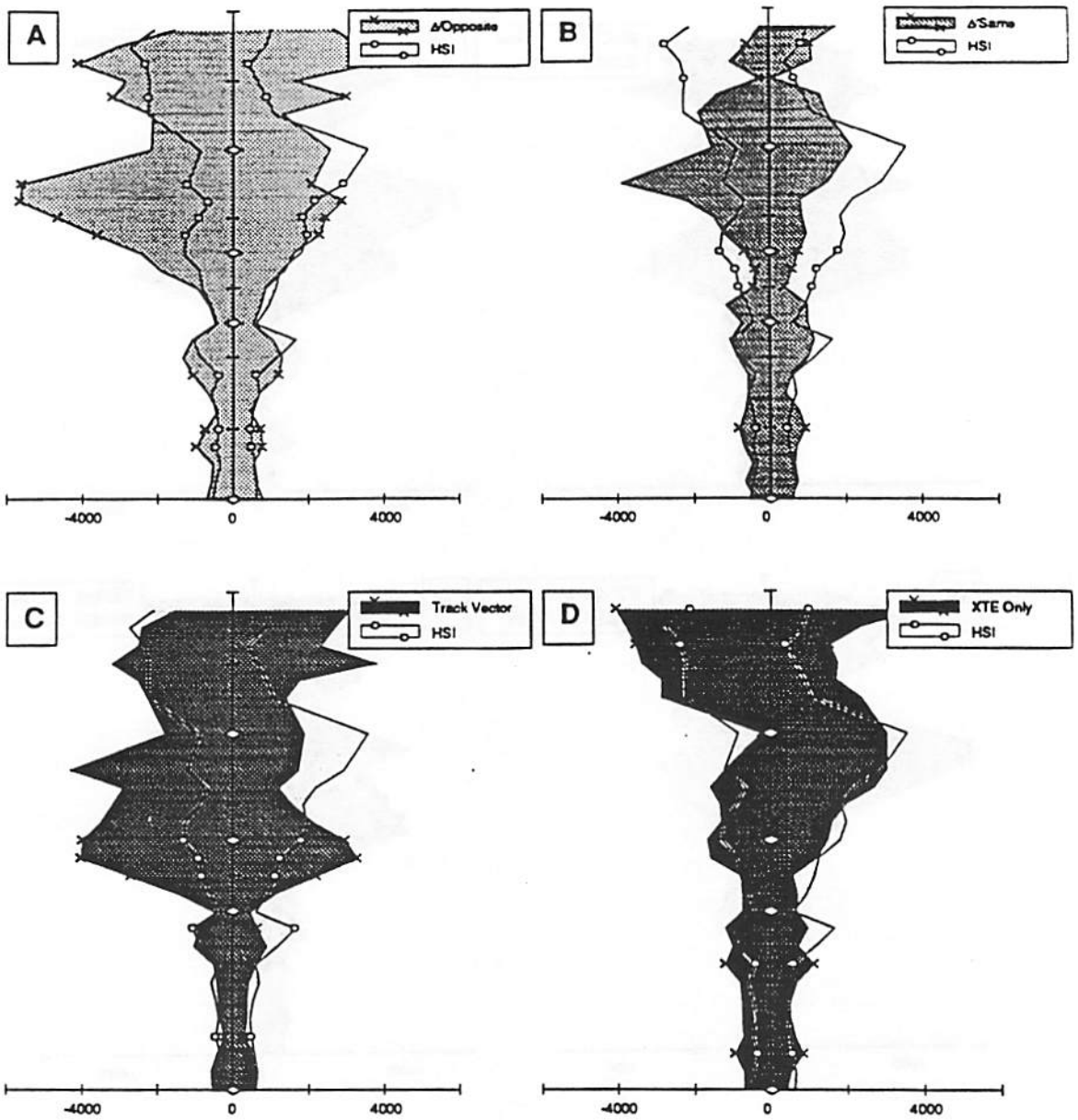


Figure 11. 95% Limits of XTE Distribution for T Approaches Only

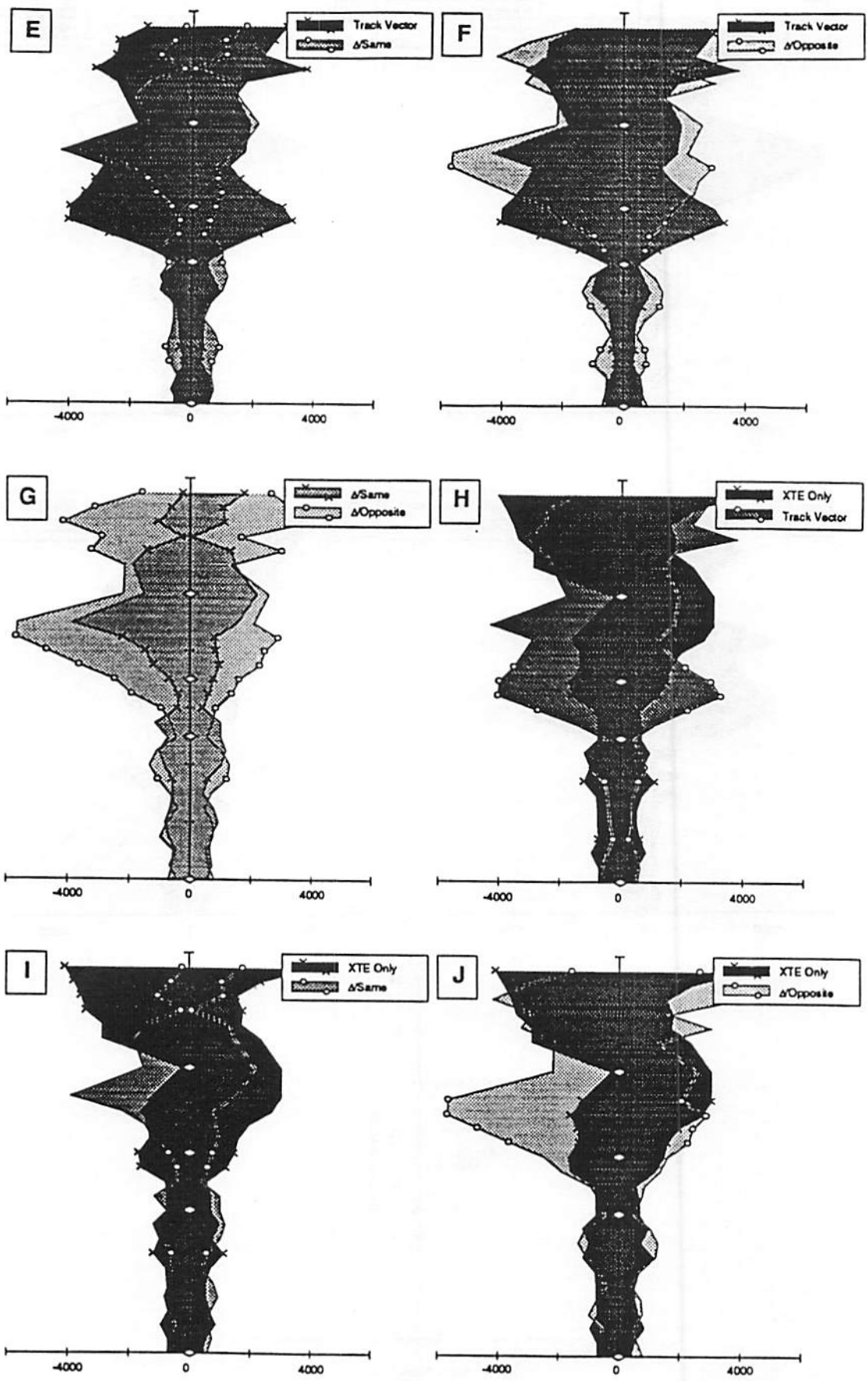


Figure 11. 95% Limits of XTE Distribution for T Approaches Only (cont.)

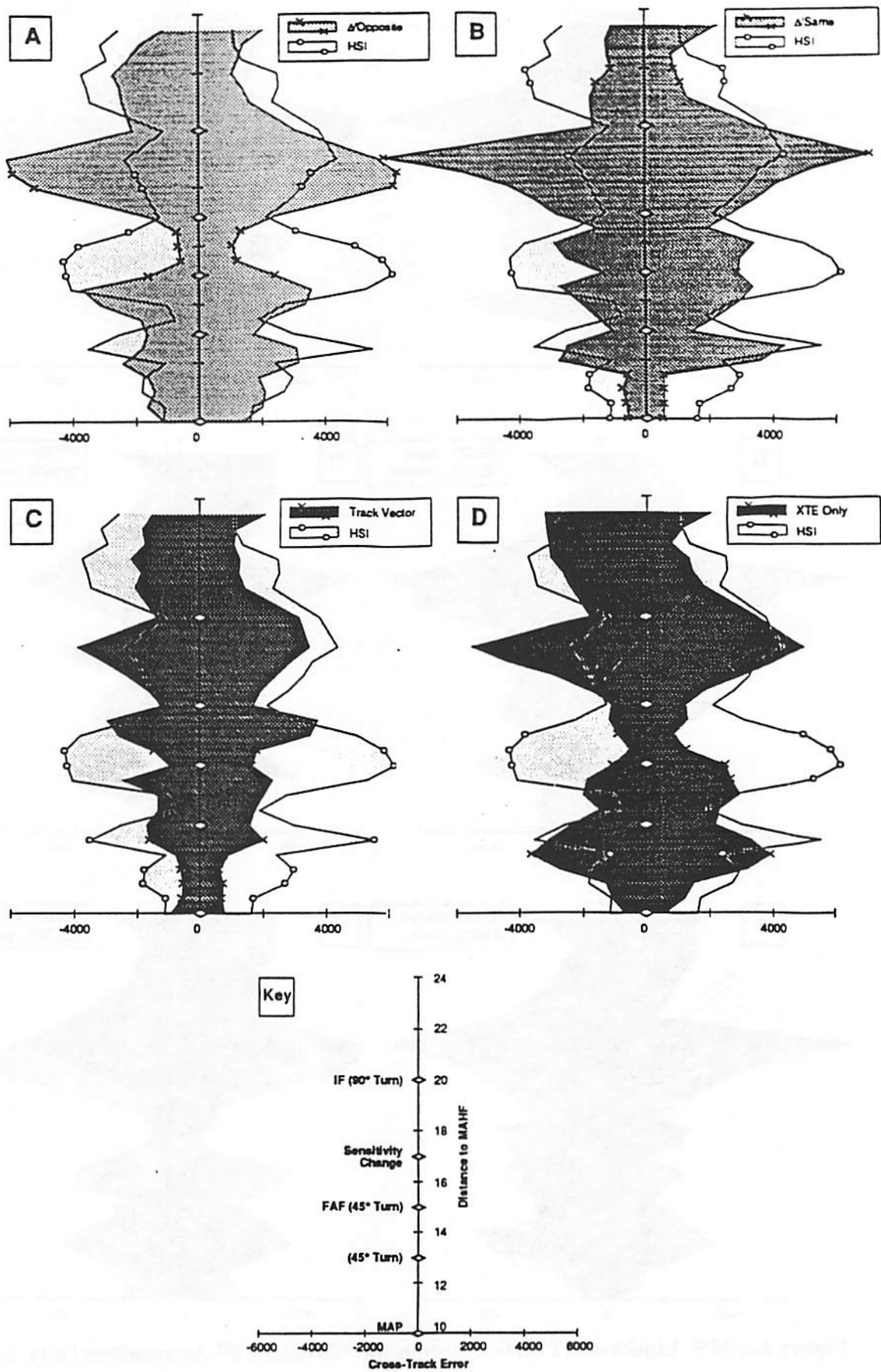


Figure 12. 95% Limits of XTE Distribution for "Crooked T" Approaches Only

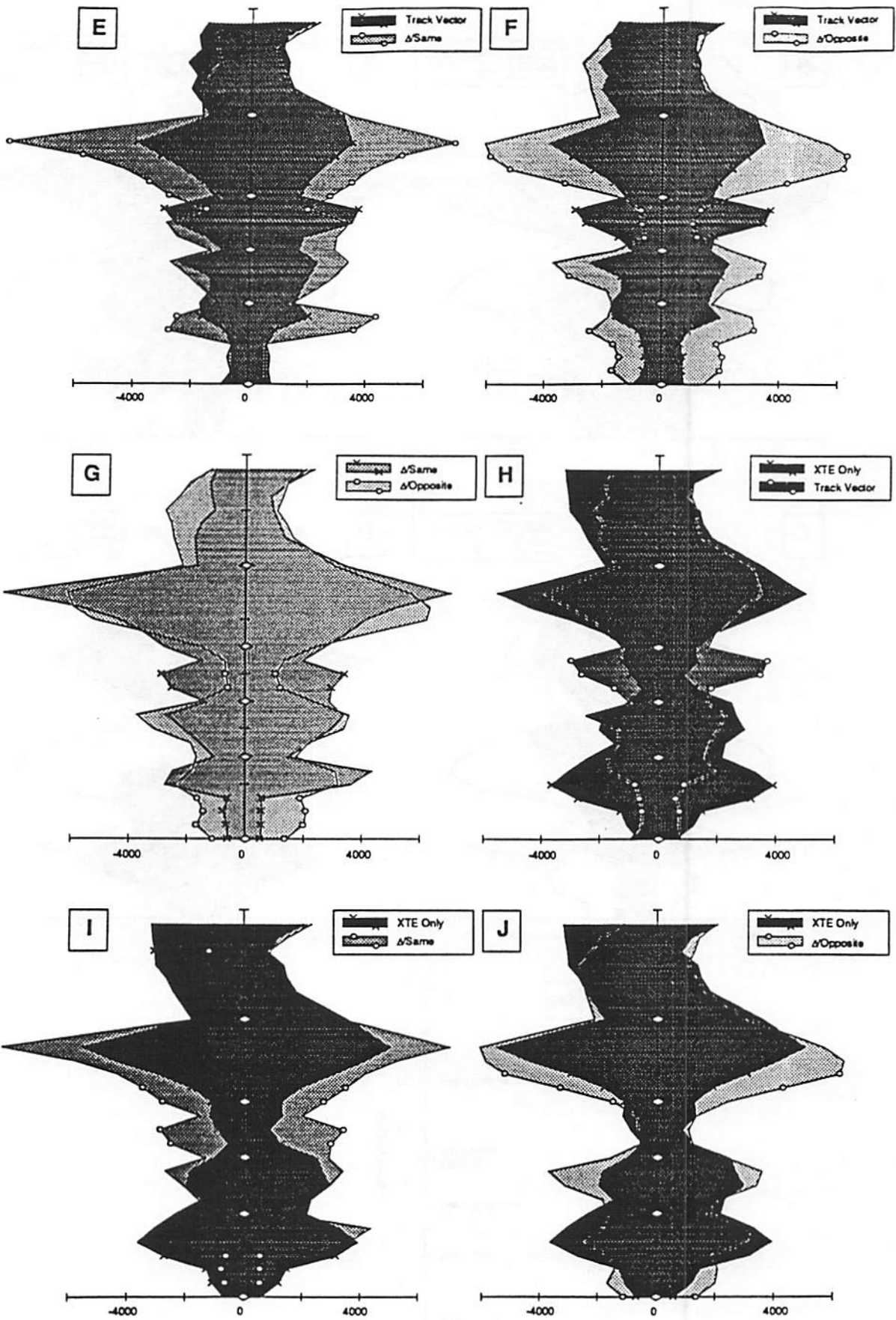


Figure 12. 95% Limits of XTE Distribution for "Crooked T" Approaches Only (cont.)

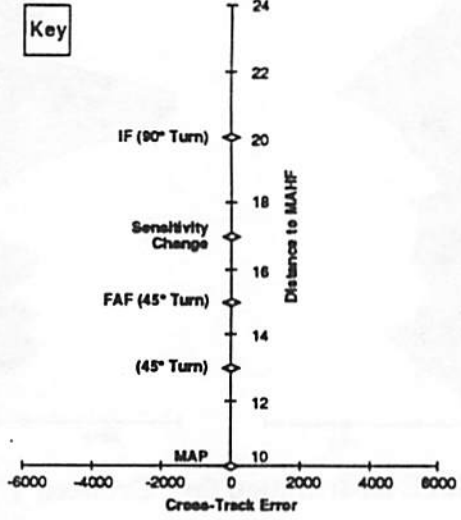
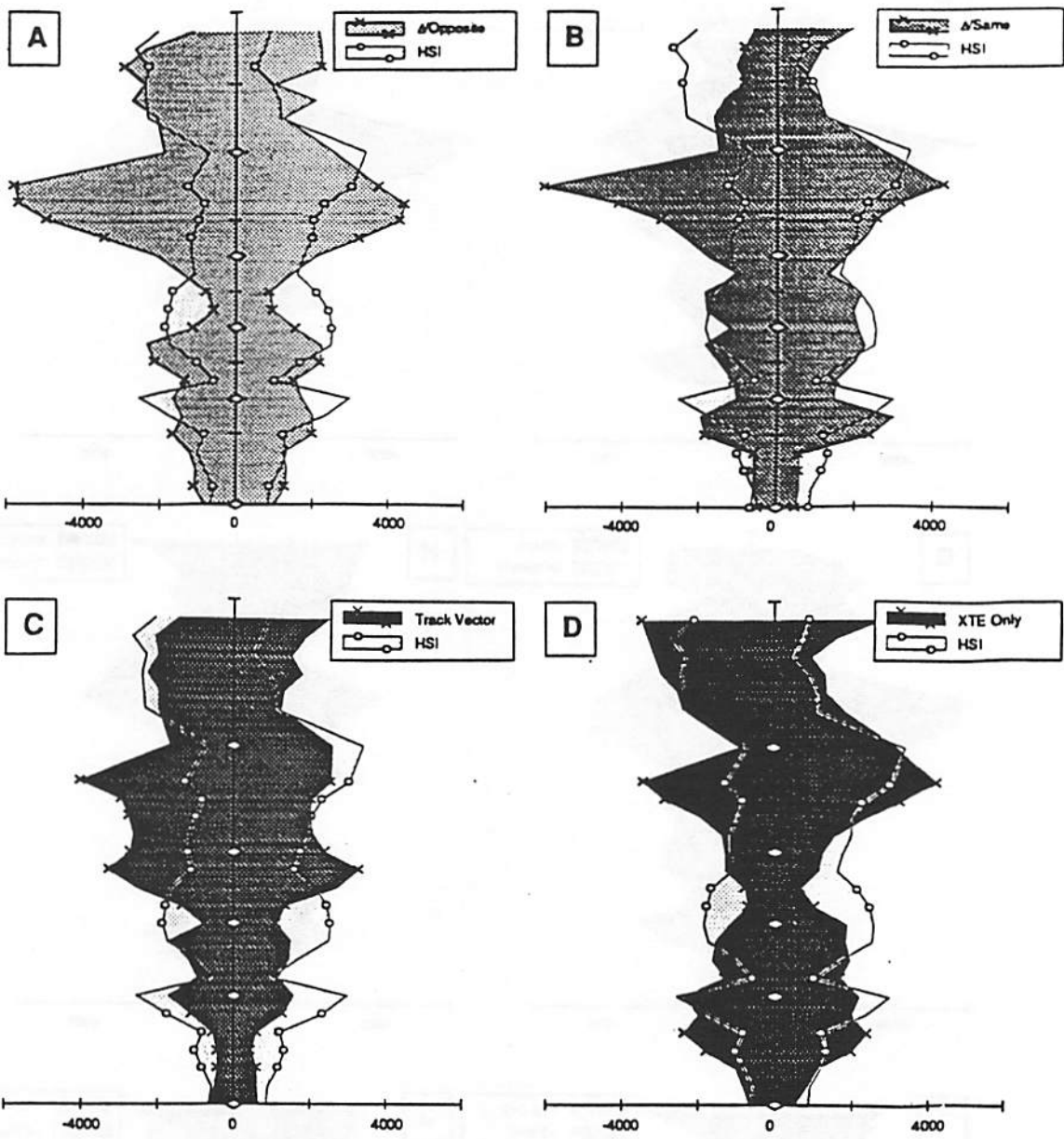


Figure 13. 95% Limits of XTE Distribution for "Crooked T" Approaches Only

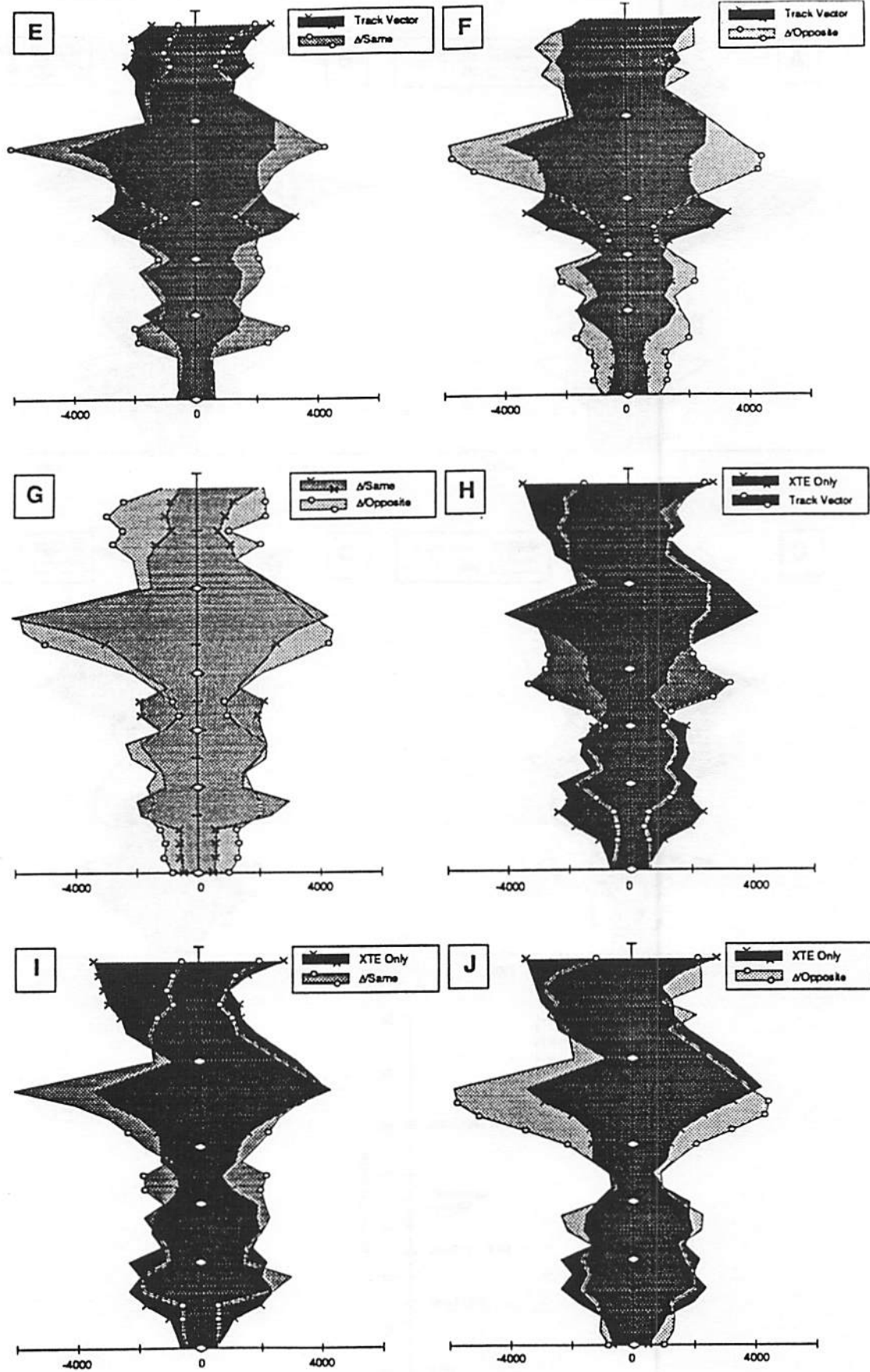
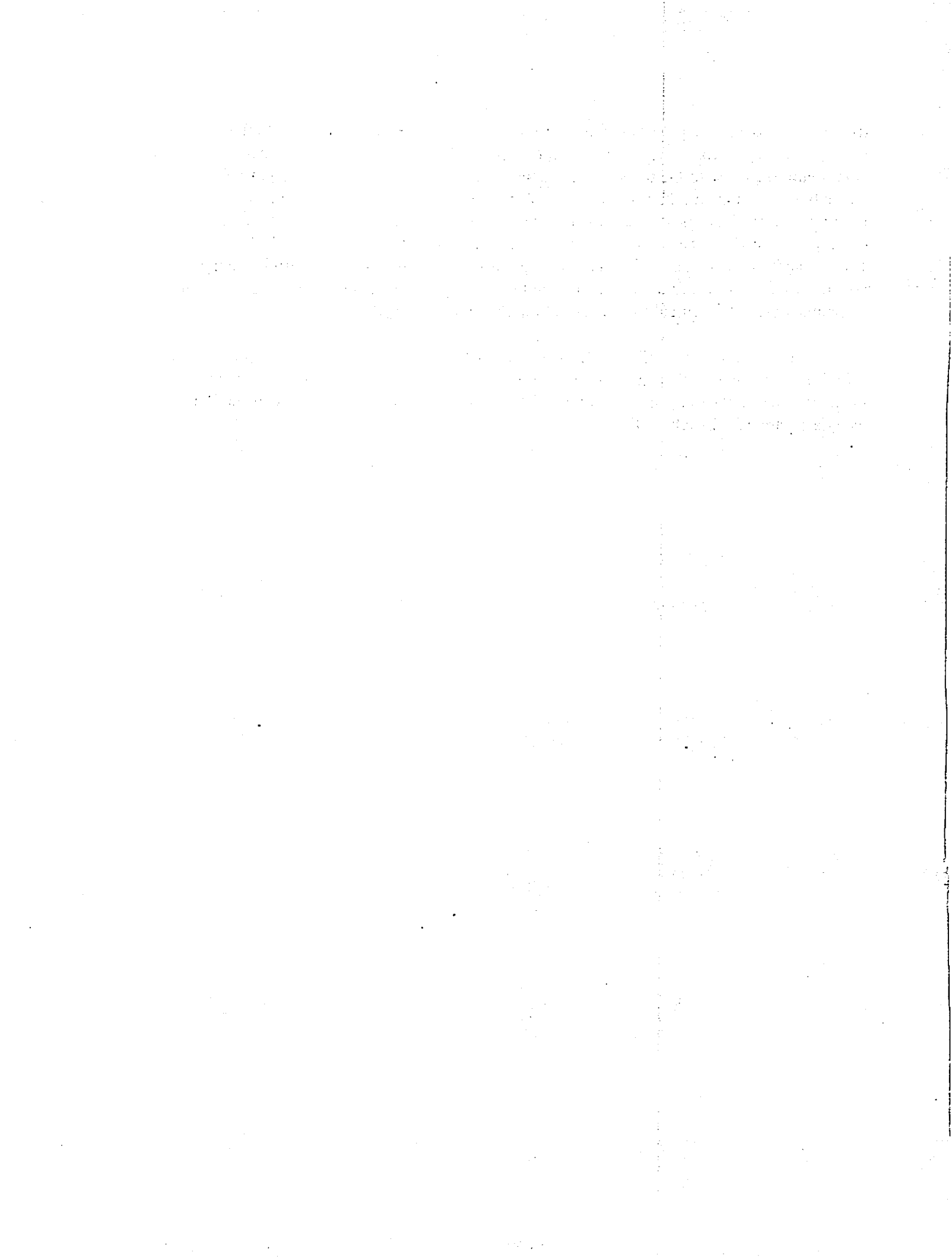


Figure 13. 95% Limits of XTE Distribution for "Crooked T" Approaches Only (cont.)

d) On the Crooked T approaches, the XTE envelopes consistently widened out after the first and second 45 deg turns. However, re-intercept performance and short final tracking was consistently better with the track vector display (Figure 12 c, e, f, and h). The track vector was the only one of the five displays for which the CDI was predicted to remain on scale through both turns in 95% of approaches flown. The next best performance was with the triangle/same display (Figure 12e). The relatively poor performance with XTE-only and HSI displays (Figures 12c, h, and Figures 12b, 12i) after 45 deg turns using high CDI sensitivity suggests clear advantages for track vector and triangle/same displays when circumstances compel pilots to maneuver during the critical final stages of an instrument approach.

The average width of the 95% XTE envelope on the last 3 miles of final approach with the "XTE-only" display in this study (0.24 nm), was qualitatively similar to that obtained during an in-flight experiment (0.32 nm, Huntley, 1993, Table 6) conducted in a Beech 55 Baron, also using a separate XTE-only CDI.



4. CONCLUSIONS

Results showed that even under turbulence conditions requiring diligent attitude instrument scan, the addition of analog TAE information to a GPS receiver XTE display significantly improved both initial and final approach leg intercept and tracking performance, probably by allowing the pilot to predict XTE changes and create outer loop control lead. Determination of wind correction angle was greatly simplified. Given the choice between analog and numeric TAE information, pilots elected not to use the numeric presentation. Thus, the findings support the FAA TSO-C129 airworthiness criteria recommendation that manufacturers provide analog TAE display capability.

Certain pilots were better able to improve their performance with TAE displays than others. However, for the group of six pilots, the "triangle/same" TAE display — a sliding TAE pointer located beneath the XTE CDI which moved in the same direction as aircraft bank — produced the largest initial leg intercept and tracking performance improvement, and was preferred overall by the pilots for flight path control. An integrated XTE/TAE "track vector" display produced the largest reduction (35%) in the width of the XTE envelope during the last three miles of final approach, as compared to control tests with XTE-only display. The track vector display could be visualized as a track up moving map, but pilots occasionally had difficulty maintaining the map interpretation, particularly immediately after waypoint changeover following a 90 deg turn. There is reason to think performance with this format may be improved by making it appear more map-like. Control testing with a horizontal situation indicator which displayed heading and XTE (but not TAE) in the center of the primary instrument panel demonstrated that the performance advantages of adding TAE to the receiver display was partly offset by the resulting widening of the pilot's instrument scan. This problem can likely be mitigated by simultaneously displaying XTE on the HSI and XTE/TAE information on the GPS receiver, but this has not yet been demonstrated.

Although Bedford workload scores were sensitive to approach geometry, no consistent effect of display format on workload was found. It is possible that our pilots adjusted their own performance criteria so that workload remained approximately constant, and performance varied instead.

5. REFERENCES

- Clement, W.F., Jex, H.R., Graham, D. (1968). A Manual Control-Display Theory Applied to Instrument Landings of a Jet Transport. *IEEE Trans. Man Machine Sys.* 9:4 93-110.
- Etkin, B. (1980). The turbulent wind and its effect on flight. *AIAA Aircraft Systems Meeting*, Anaheim, CA, AIAA-80-1836.
- Federal Aviation Administration (1994). Technical Standard Order C129: Airborne Supplemental Navigation Equipment Using the GPS. FAA, Washington, DC.
- Huntley, M.S. Jr. (1993). Flight Technical Error for Category B Non-Precision Approaches and Missed Approaches Using Non-Differential GPS for Course Guidance. Report DOT-VNTSC-FAA-93-17.
- Jansen, C.J. "Non-Gaussian Atmospheric Turbulence Model for Flight Simulator Research." *AIAA J. Aircraft* 19 (1981): 374-379.
- Roscoe, A.H. and Ellis, G.A. (1990). A subjective rating scale for assessing pilot workload in flight. Tech. Report TR90019, RAE Farnborough, UK.
- RTCA Special Committee 15. (1991). Minimum Operational Performance Standards For Airborne Supplemental Navigation Equipment Using Global Positioning System, DO-208 July, 1991, 1140 Connecticut Avenue, N.W., Washington, DC.
- Van de Moesdijk, G.A.J. (1978). Non-Gaussian structure of the simulated turbulent environment in piloted flight simulation. Delft University of Technology, Memorandum M-304.

1. The first part of the document discusses the importance of maintaining accurate records of all transactions and activities. It emphasizes that this is essential for ensuring transparency and accountability in the organization's operations.

2. The second part of the document outlines the various methods and tools used to collect and analyze data. It highlights the need for consistent data collection procedures and the use of advanced analytical techniques to derive meaningful insights from the data.

3. The third part of the document focuses on the role of technology in data management and analysis. It discusses how modern software solutions can streamline data collection, storage, and processing, thereby improving efficiency and reducing the risk of errors.

4. The fourth part of the document addresses the challenges associated with data security and privacy. It stresses the importance of implementing robust security measures to protect sensitive information and ensure compliance with relevant regulations.

5. The fifth part of the document provides a summary of the key findings and recommendations. It concludes that a comprehensive data management strategy is crucial for the organization's success and that ongoing monitoring and evaluation are necessary to ensure its effectiveness.

APPENDIX A-1: FLIGHT SIMULATOR, COMPUTER NETWORK, TURBULENCE, AND WIND MODELS

Volpe FRASCA 242 Research Flight Simulator and Computer Network:

The simulator used for this study was a modified Frasca Model 242 convertible flight training device. The fixed base, two-seat enclosed cockpit is equipped with dual yoke and rudder pedals, and an instrument panel shown schematically in Figure A1-1. Control loading varied dynamically with airspeed. A Horizontal Situation Indicator (HSI) was located immediately beneath the Attitude Indicator. Pilots were free to use the HSI course needle and heading bug as memory aids, at their own discretion. GPS displays were presented on a 10-inch diagonal color active matrix LCD Flat Panel Display installed to the right of the primary instrument panel. The aircraft was equipped with simulated dual 720 channel navcomm radios, headsets, and intercom. Simulated VOR/ILS/ADF avionics and an autopilot with flight director were also available, but not utilized in the present experiment.

The Frasca 242 simulator uses a Zendex 80386-based digital Simulation Computer running flight system software (Frasca X4X EPROM version 1.11), which models the flight dynamics of the aircraft, determines its position, and drives the conventional cockpit instruments, avionics, yoke, and autopilot. Aircraft flight characteristics are determined by aerodynamic model performance constants which can be changed via the operator console. The set of model constants used had been developed by the manufacturer to resemble the performance of a Piper Aztec.

As shown in Figure A1-2, seven additional 80386 computers were used to extend the capability of the simulator. These computers ran program modules written in Visual Basic, and communicated with one another and to the Volpe Center computer network and file servers via a local area network (Ethernet/Windows for Workgroups/Novell Netware). The seven computers are designated by the function of their resident software modules.

The Simulation Control Console ("runcon") module permitted the user to select an approach geometry, to monitor the status of the other computers, and to provide a data recording facility. It also allowed various flight variables to be monitored during a simulation. All the data distributed around the system was collected and stored in memory for later storage in the network data archive. The position of the aircraft was also plotted on a user display for monitoring purposes.

The data server provided the link to the Frasca simulation computer. It is used to initialize the simulation computer prior to each approach, read the various state variables from the simulator and distribute them to the other computers via Windows Dynamic Data Exchange (DDE) links during each approach.

The GPS simulator monitored the simulated latitude/longitude position read by the data server, and calculated ground speed, cross track error and track angle error based on flight plan parameters. The waypoints of the flight plan are stored on a common Microsoft Access Database and the Control Console told the GPS simulator program which plan to use. The GPS data calculated were distributed via Network DDE links read by the Control Console, the Flat Panel Display Controller and the Instrument Server.

Cockpit Layout

FRASCA 242

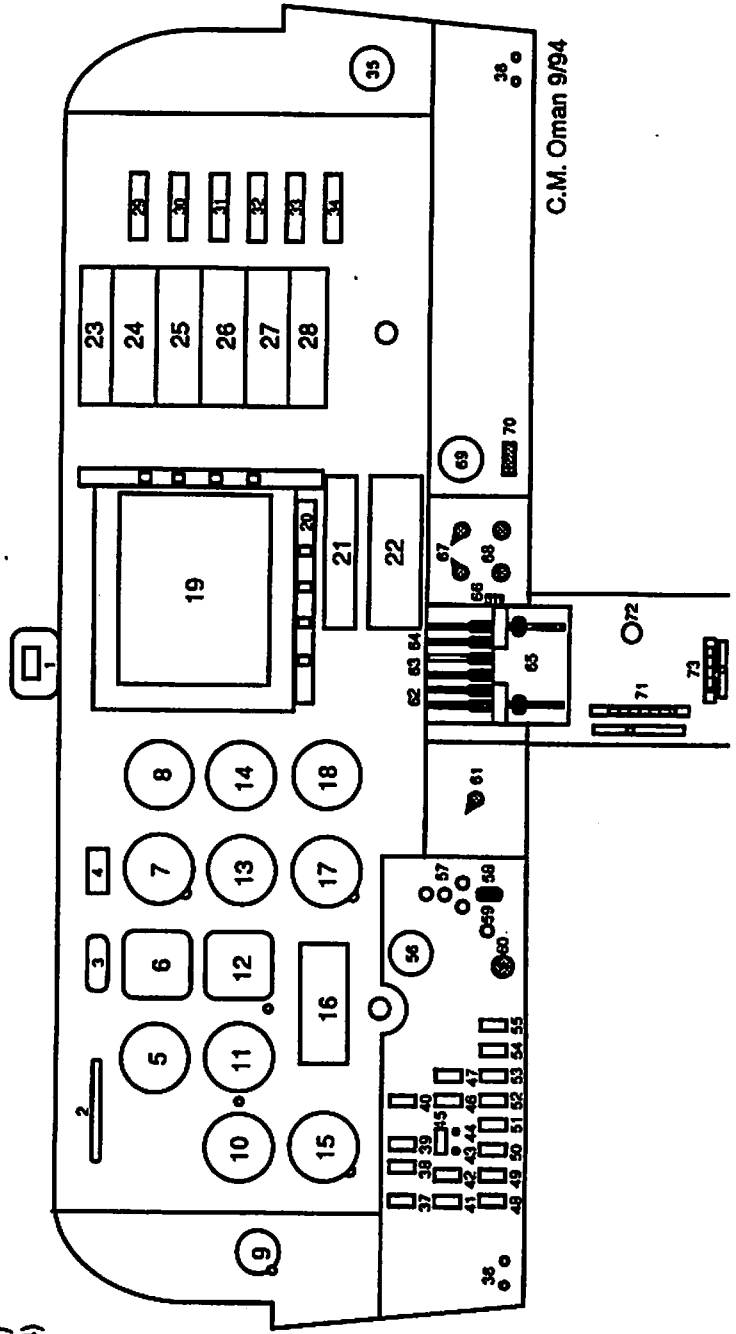
Research Flight Simulator

Cockpit Human Factors Program

Volpe National Transportation Systems Center

1. Magnetic compass
2. GPS annunciator panel
3. DME display
4. Intercom control (PM 1000)
5. Airspeed indicator
6. Altitude indicator (King Flight Command Indicator)
7. Pressure altimeter
8. Dual manifold pressure indicator
9. Clock
10. Automatic direction finder (dual needle RMI)
11. Turn coordinator
12. Horizontal situation Indicator (King PNI)
13. Vertical velocity indicator
14. Dual tachometer
15. VHF navigation dual needle ILS CDI
16. LCD display (research)
17. VHF navigation dual needle ILS CDI
18. Fuel flow indicators
19. Flat panel display (research)
20. Selector button bar (research)
21. Autopilot (King KFC-150)
22. GPS receiver (II Morrow Apollo 2001NMS)
23. Marker beacon/audio switch (King KMA24)
24. VHF NAVCOM 1 transceiver
25. VHF NAVCOM 2 transceiver
26. Automatic direction finder receiver
27. Mode C radar transponder
28. Distance measuring equipment
29. Fuel quantity indicators
30. Fuel pressure indicators
31. Oil pressure indicators
32. Oil temperature indicators
33. Cylinder head temperature indicators
34. Electrical load meters
35. Hourmeter
36. Microphone and headphone jacks
37. Master switch
38. Left generator switch
39. Right generator switch
40. Avionics master switch
41. Left engine left magneto switch
42. Left engine right magneto switch
43. Left engine primer button
44. Right engine primer button
45. Starter switch

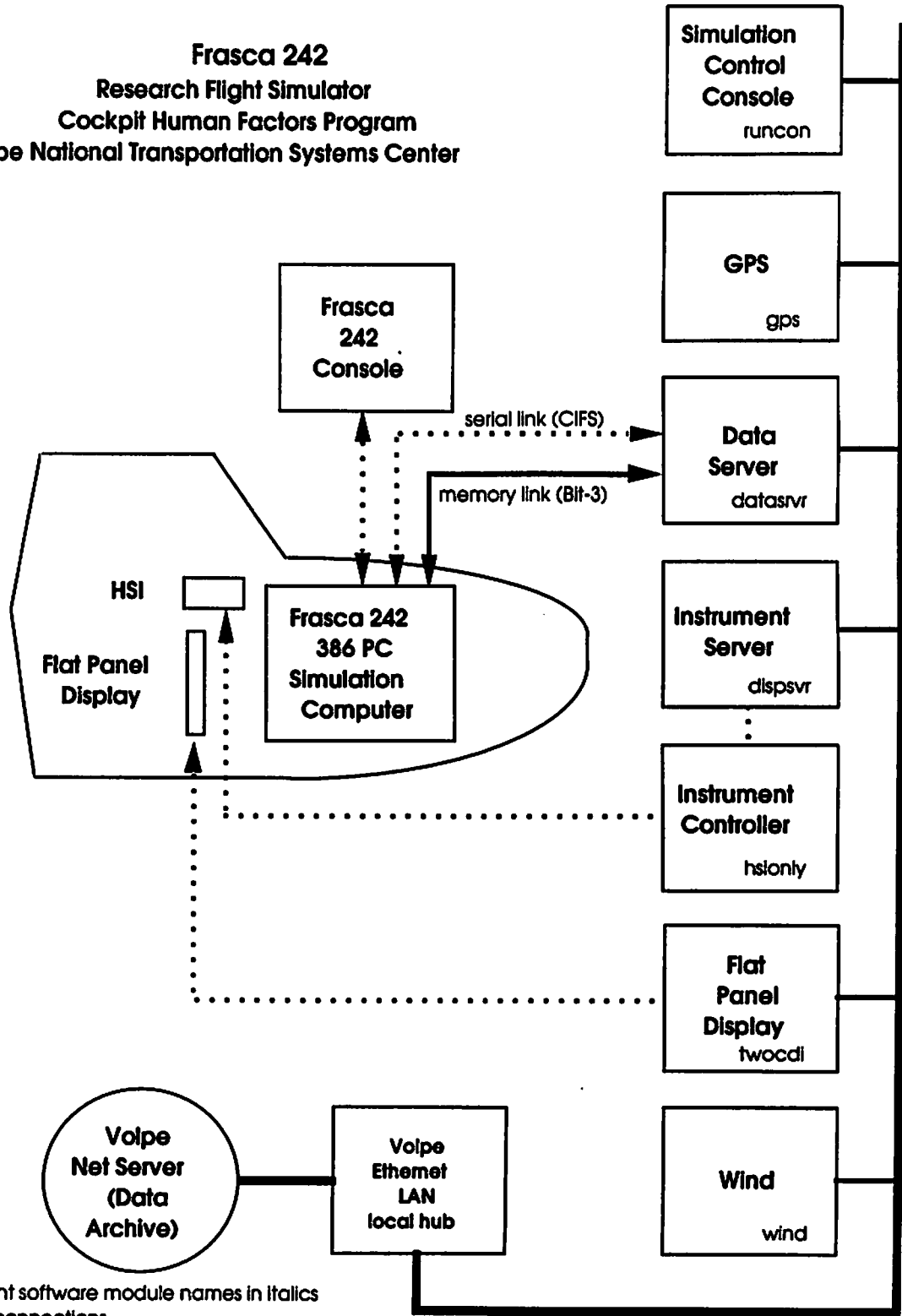
46. Right engine left magneto switch
47. Right engine right magneto switch
48. Left landing light switch
49. Right landing light switch
50. Navigation position light switch
51. Anti-collision light switch
52. Pitot heat switch
53. Left fuel boost pump switch
54. Right fuel boost pump switch
55. Rotating beacon switch
56. Pneumatic system pressure indicators
57. Landing gear position indicator lights
58. Landing gear control lever
59. Landing gear warning horn silencer button
60. Parking brake control knob
61. Flat panel display intensity rheostat
62. Throttle controls
63. Propeller controls
64. Mixture controls
65. Carburetor heat controls
66. Throttle quadrant friction adjustment knob
67. Fuel tank selector valves
68. Cowl flap controls
69. Wing flaps % position indicator
70. Wing flaps control lever
71. Elevator trim wheel and position indicator
72. Aileron trim control and position indicator
73. Rudder trim control and position indicator



C.M. Oman 9/94

Figure A1-1. FRASCA 242 Research Flight Simulator: Cockpit Layout

Frasca 242
Research Flight Simulator
Cockpit Human Factors Program
Volpe National Transportation Systems Center



resident software module names in *italics*
 serial connections
 10 base T Ethernet connections ———

Figure A1-2. Frasca 242 Research Flight Simulator

The Wind Simulator continuously updated the local wind speed and direction used by the Frasca computer based on aircraft altitude, using a model described below.

The Flat Panel Display Controller drove the Flat Panel Display used to show the GPS receiver displays employed in the present experiment.

The Instrument Server and Instrument Controller computers commanded certain other analog instruments and displays, including the CDI needle located on the HSI instrument. The Instrument Server program received digital CDI needle commands via Network DDE links and sent them via a Serial RS232 link to the Instrument Controller, which in turn drove the CDI via a D/A converter.

Wind Model

The atmospheric wind model interpolated values for wind upward from the surface through a given value at a reference height ("atmospheric boundary layer thickness"), assuming that wind speed increases exponentially with height above ground (Etkin, 1980), and that the near-ground exponent depends on ground roughness.

The model used assumed that if

h = aircraft altitude above ground level (ft)

U = wind velocity at altitude h (ft/sec)

δ = atmospheric boundary layer thickness (assumed to be 3000 ft in this simulation)

U_{δ} = wind at $h = \delta$

R = ground roughness height (assumed to be 20 ft for this simulation)

U_0 = wind at ground level (ft/sec)

$$U = U_0 + (U_{\delta} - U_0)(h/\delta)^{\alpha}$$

if $0 \leq h \leq \delta$, then $\alpha = 0.0072R + 0.14$

if $h > \delta$, then $\alpha = 0.35$

Non-Gaussian Atmospheric Turbulence Model:

Patchy turbulence was created by adding disturbance signals to the Frasca simulator's roll and pitch angles, and rate of change of heading at 30 Hz. Separate turbulence generator models were used on each of the three axes, coded in the simulator EPROM for us by Frasca International. The model employed is based on the NLR method (Jansen, 1981; Van de Moesdijk, 1978), and is documented below:

The turbulence disturbance signal $d(t)$ on a given axis is the product of an axis gain factor, K , and a unity variance signal $w(t)$. The power spectrum of $w(t)$ is determined by a characteristic time constant τ , equal to the ratio of turbulence scale length to airspeed, L/V . The user sets a

“patchiness intensity factor” Q , which determines the degree to which the signal $w(t)$ departs from a Gaussian distributed signal ($Q=0$) toward a Bessel distributed signal ($Q=\infty$). Thus, characteristic patch length = L/R , and characteristic patch duration is L/VR .

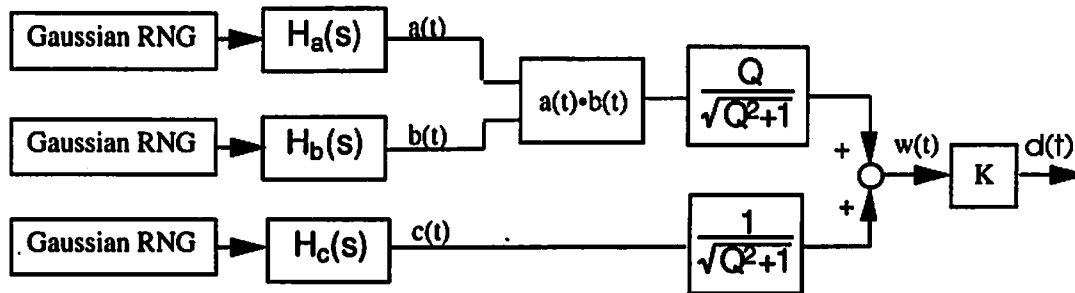


Figure A1-3. Turbulence Synthesis Method

To derive $w(t)$, a Gaussian, band-limited, unity variance random signal $a(t)$ was created by using a unity variance, Gaussian distributed random number generation (RNG) routine to derive a 30 Hz white noise signal. As shown in Figure A1-3, this was then filtered by a first order low pass shaping filter $H_a(s)$, whose gain was chosen so the resulting signal, $a(t)$, had unity variance. The result, $a(t)$, was multiplied by a second Gaussian process $b(t)$, formed in a similar way with a second RNG and shaping filter. $b(t)$ had a lower band-width, determined by a “patch length factor,” R , which varied from 1 to 0. The product $a(t) \cdot b(t)$ was a unity variance, Bessel distributed random process. Separately, a third RNG and shaping filter was used to create a “baseline” Gaussian process $c(t)$. The two signals $a(t) \cdot b(t)$ and $c(t)$ were blended together using functions of a “patchiness intensity” parameter Q so that the variance of the resulting sum, $w(t)$, had a unity variance independent of Q . The value of R did not affect the power spectrum or the probability density function of $w(t)$.

So:

$$w(t) = a(t) \cdot b(t) \frac{Q}{\sqrt{Q^2 + 1}} + c(t) \frac{1}{\sqrt{Q^2 + 1}}$$

where $a(t)$ is a Gaussian output of filter H_a , $b(t)$ is the patchiness modulator output of filter H_b , and $c(t)$ is the purely Gaussian output of filter H_c .

Filter transfer functions $H_{a,b,c}$ are:

$$H_{a,b,c}(s) = \frac{K_{a,b,c}}{1 + \tau_{a,b,c}s}$$

Where:

$$\tau_a = \tau(R + 1)$$

$$\tau_b = \tau(R + 1)/R$$

$$\tau_c = \tau = L/V$$

and

$$K_{a,b,c} = \sqrt{2\pi^2 \tau_{a,b,c}}$$

The turbulence magnitude on each axis was set by a turbulence gain parameter. Band-width and statistical characteristics on each axis were adjusted using three other parameters. For purposes of our simulation, the roll turbulence scale L was set at 500 ft, and the characteristic patch length at 2500 ft, so the characteristic roll axis patch duration was 12.5 seconds. The pitch turbulence scale was 200 ft. Since the patch length was 4-10 times shorter than any of the approach segments evaluated, RMS turbulence parameters were essentially constant across approaches. The ratio of roll/pitch/yaw RMS disturbance was 15/5/1 times, respectively. The effect of adding patchiness to the roll disturbance is illustrated in Figure A1-4 below (Top: $Q=5$; Bottom, $Q=0$).

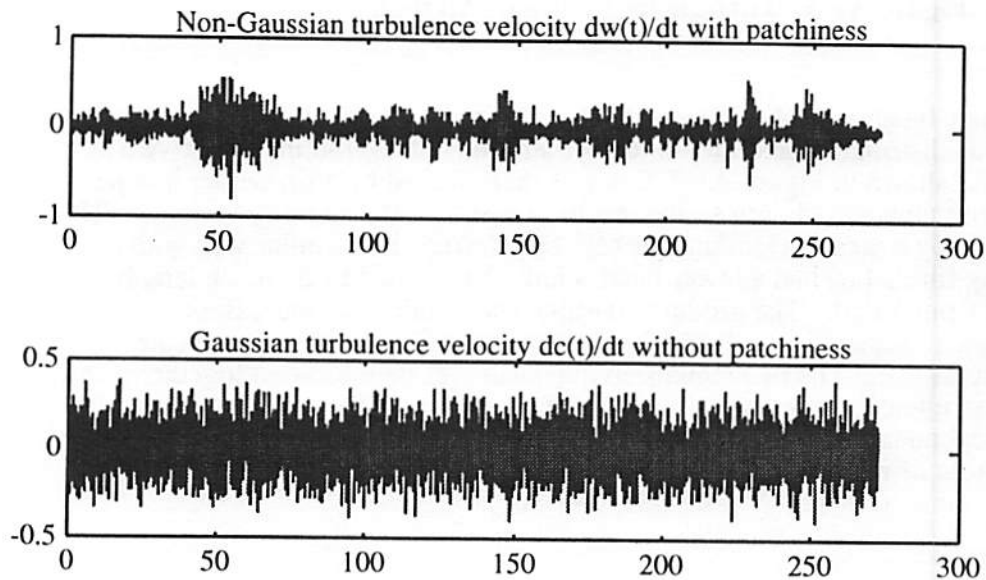


Figure A1-4. Example of Turbulence Disturbance Signals

APPENDIX A2 - APPROACH CHARTS

Figures A2-1 through 8: The eight simulated GPS non-precision approach charts to fictitious airports used in the experiment:

“T” Approaches:

Figure A2-1: Bathurst (BTA) Runway 24

Figure A2-2: Coffs Harbour (CFB) Runway 6

Figure A2-3: Condobolin (CDN) Runway 34

Figure A2-4: Tamworth (TMA) Runway 16

“Crooked T” Approaches:

Figure A2-5: Cadney Park (CPA) Runway 28

Figure A2-6: Dalhousie Springs (DHS) Runway 10

Figure A2-7: Mudgee (MDG) Runway 13

Figure A2-8: Warnambool (WMB) Runway 31

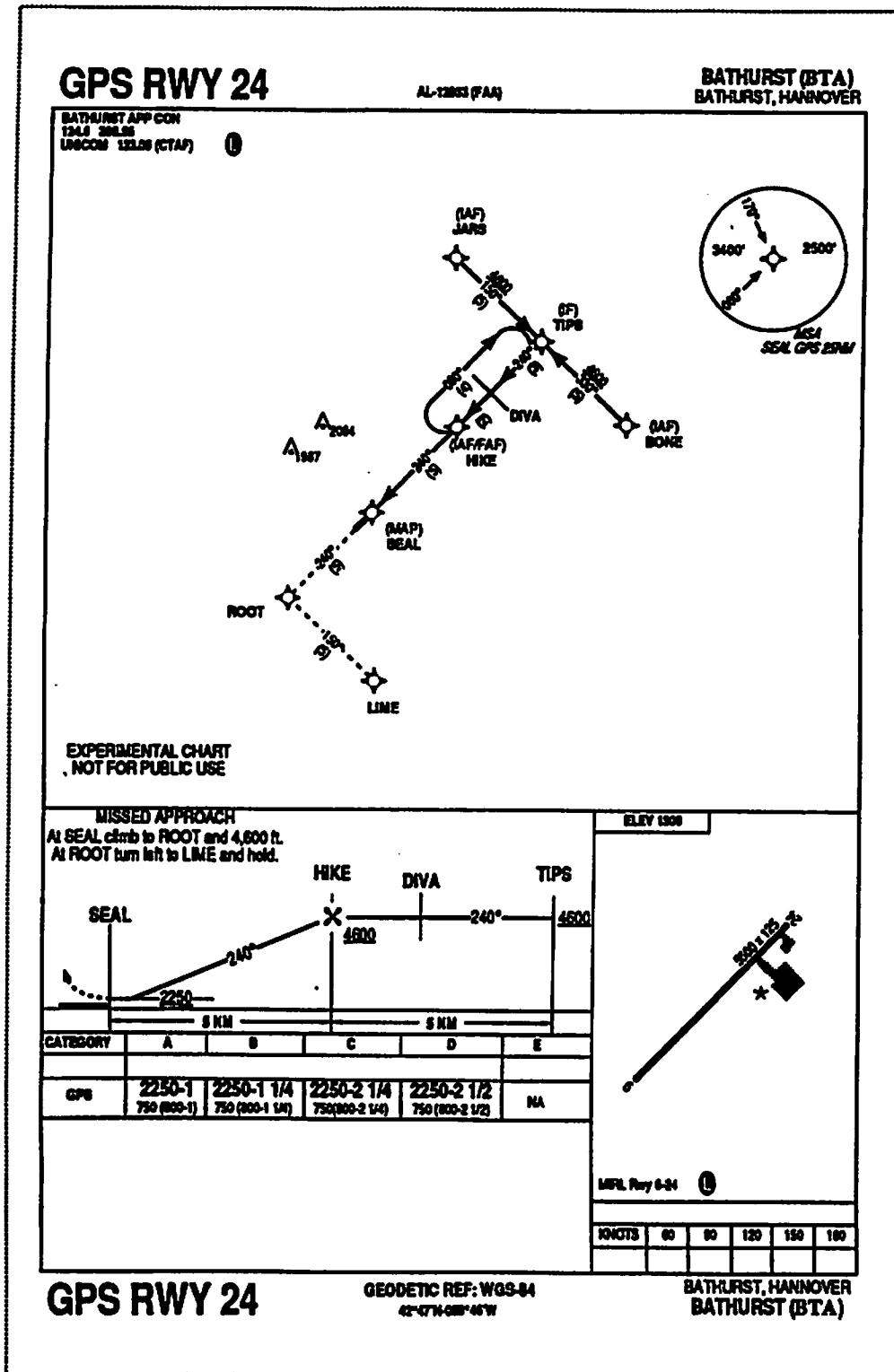


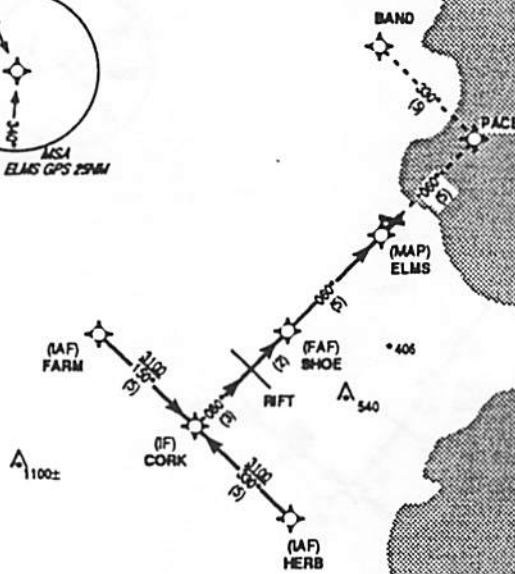
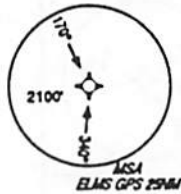
FIGURE A2-1. BATHURST (BTA) RUNWAY 24

GPS RWY 6

AL-31042 (FAA)

COFFS HARBOUR (CFB)
COFFS HARBOUR, HARMEN

COFFS HARBOUR APP CON
132.25 200.1
UNICOM 122.7 (CTAF)



EXPERIMENTAL CHART
NOT FOR PUBLIC USE

MISSED APPROACH
At ELMS climb to PACE and 3,100 ft.
At PACE turn left to BAND and hold.

ELEV 6

CATEGORY	A	B	C	D	E
GPS	750-1 750 (800-1)	750-1 1/4 750 (800-1 1/4)	750-2 1/4 750 (800-2 1/4)	750-2 1/2 750 (800-2 1/2)	NA

MIFL Flyer 6-24

KNOTS	80	90	120	150	180

GPS RWY 6

GEODETIC REF: WGS-84
42°48'N-058°32'W

COFFS HARBOUR, HARMEN
COFFS HARBOUR (CFB)

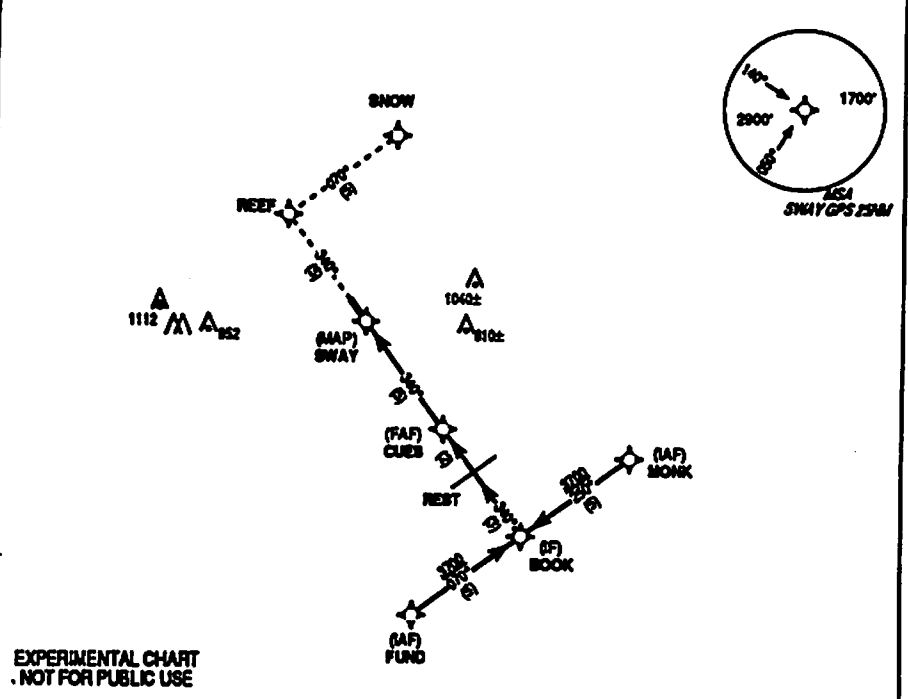
FIGURE A2-2. COFFS HARBOUR (CFB) RUNWAY 6

GPS RWY 34

AL-34281 (FAA)

CONDOBOLIN (CDN)
CONDOBOLIN, VICTORIA

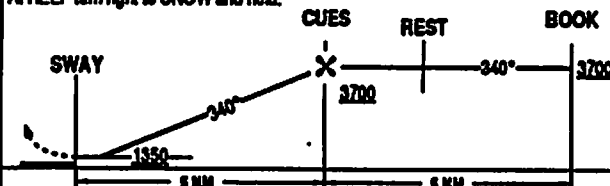
CONDOBOLIN CENTER
12L45 379.9
UNCOM 12L8 (CTAF)



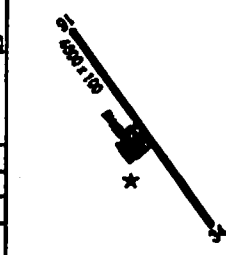
EXPERIMENTAL CHART
. NOT FOR PUBLIC USE

MISSED APPROACH

At SWAY climb to REEF and 3,700 ft.
At REEF turn right to SNOW and hold.



ELEV 686



CATEGORY	A	B	C	D	E
GPS	1350-1 750 (R00-1)	1350-1 1/4 750 (R00-1 1/4)	1350-2 1/4 750 (R00-2 1/4)	1350-2 1/2 750 (R00-2 1/2)	NA

MPL Rwy 16-34

RWYTS	80	80	120	150	180

GPS RWY 34

GEOIDETIC REF: WGS-84
42°47'N 089°21'W

CONDOBOLIN, VICTORIA
CONDOBOLIN (CDN)

FIGURE A2-3. CONDOBOLIN (CDN) RUNWAY 34

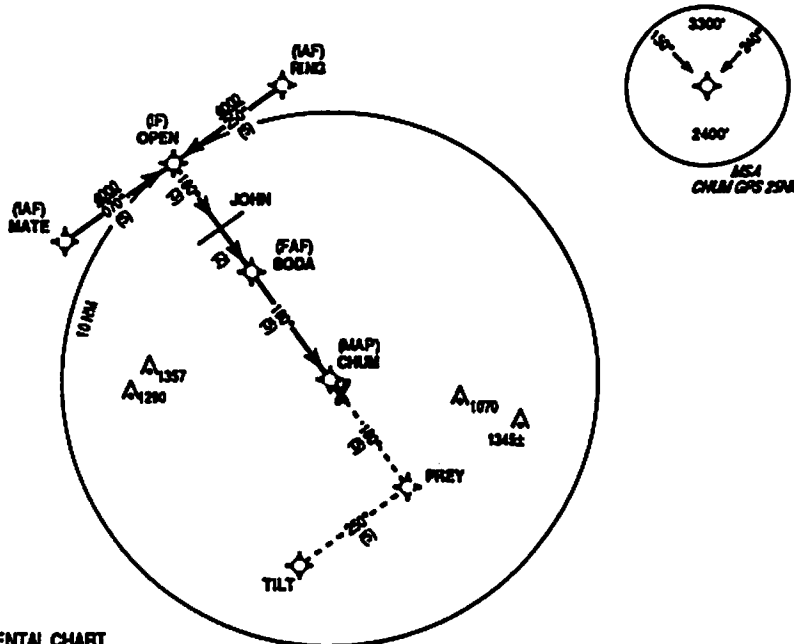
GPS RWY 16

AL-03018 (FAA)

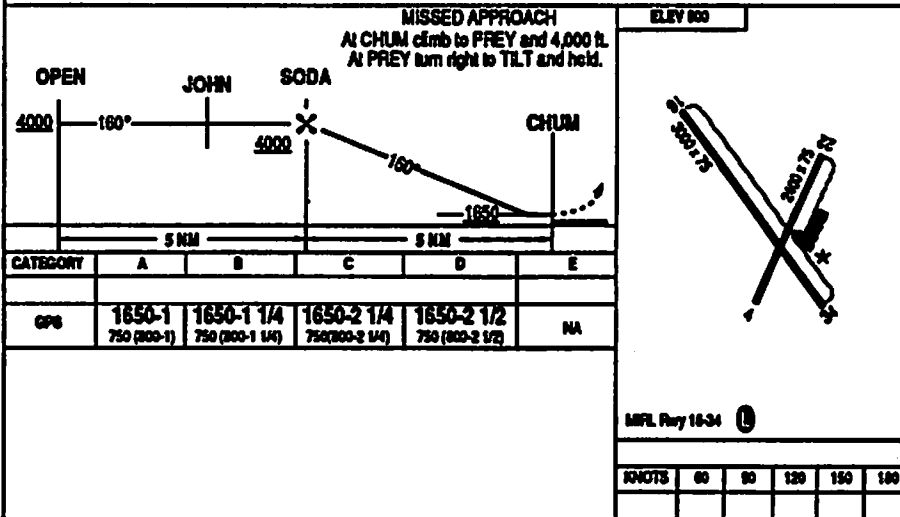
TAMWORTH (TMA)
TAMWORTH, HARMEN

TAMWORTH CENTER
SIDES 377.1
UNCOM 122.8 (CTAF)

①



EXPERIMENTAL CHART
NOT FOR PUBLIC USE



GPS RWY 16

GEOCETIC REF: WGS-84
42°47'48" N 01°28'37" W

TAMWORTH, HARMEN
TAMWORTH (TMA)

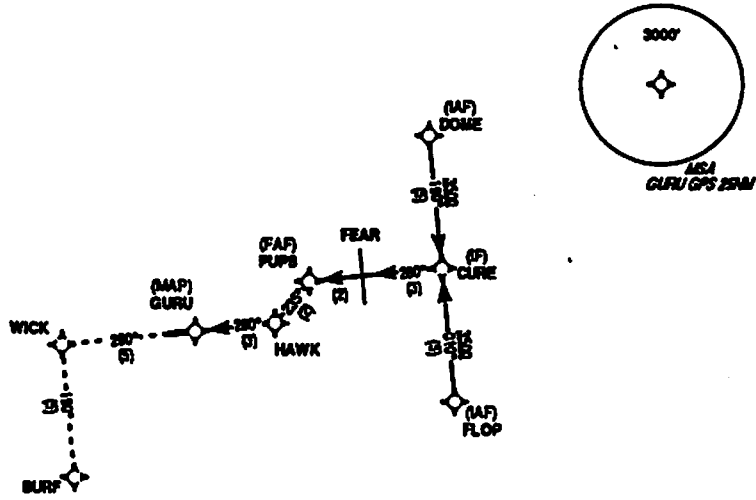
FIGURE A2-4. TAMWORTH (TMA) RUNWAY 16

GPS RWY 28

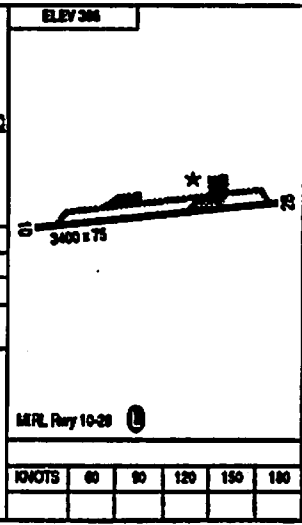
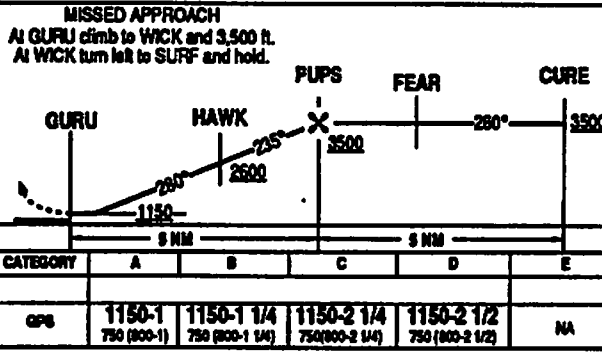
AL-4275 (FAA)

CADNEY PARK (CPA)
CADNEY PARK, CARMEL

CADNEY PARK CENTER
127.4 368.8
UNCOM 122.875 (CTAF) **(L)**



EXPERIMENTAL CHART
NOT FOR PUBLIC USE



GPS RWY 28

GEODETIC REF: WGS-84
43°53'N 089°13'W

CADNEY PARK, CARMEL
CADNEY PARK (CPA)

FIGURE A2-5. CADNEY PARK (CPA) RUNWAY 28

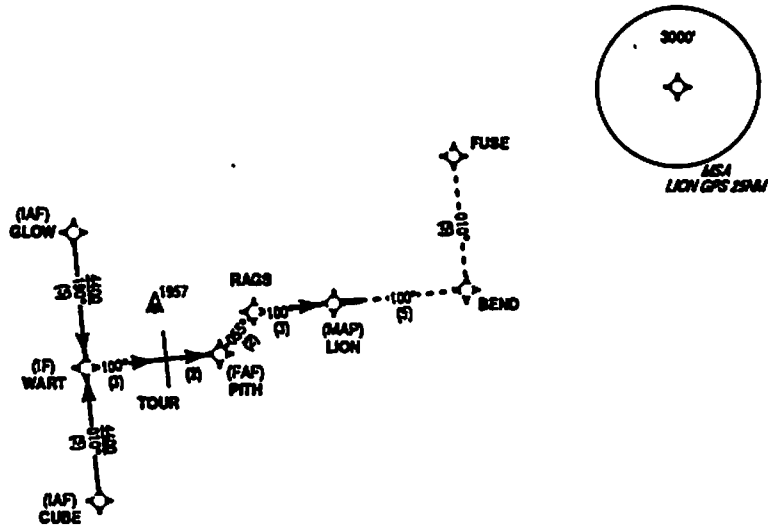
GPS RWY 10

AL-8796 (FAA)

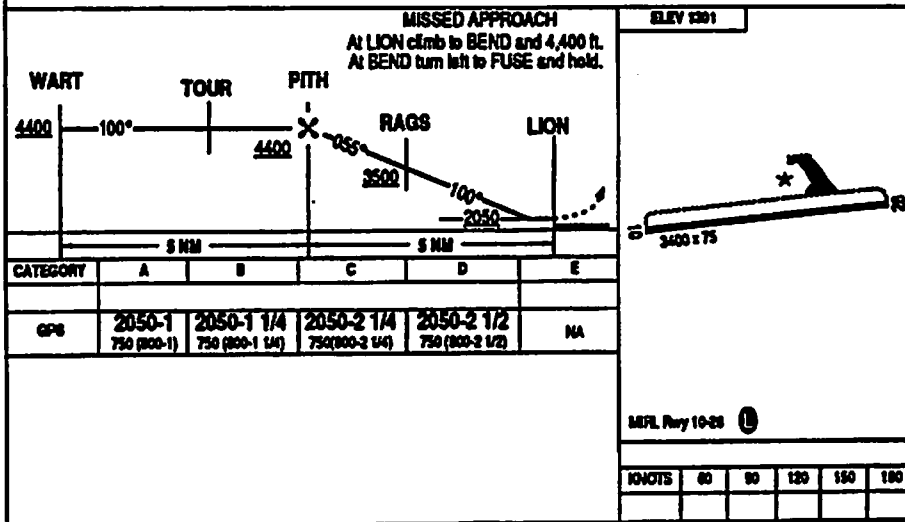
DALHOUSIE SPRINGS (DHS)
DALHOUSIE SPRINGS, RYDALMERE

INDIANKA CENTER
126.3 204.1
UNCOM 122.9 (CTAF)

①



EXPERIMENTAL CHART
NOT FOR PUBLIC USE



GPS RWY 10

GEODEIC REF: WGS-84
42°37'N 159°15'W

DALHOUSIE SPRINGS, RYDALMERE
DALHOUSIE SPRINGS (DHS)

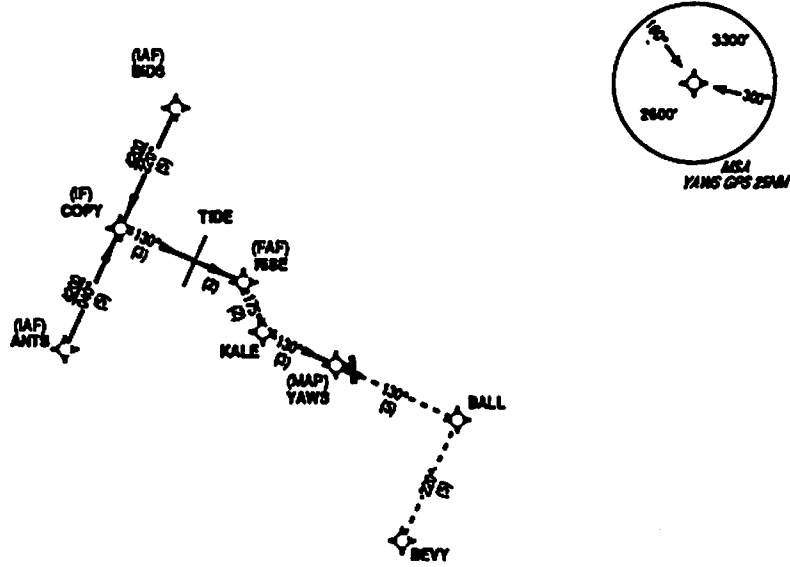
FIGURE A2-6. DALHOUSIE SPRINGS (DHS) RUNWAY 10

GPS RWY 13

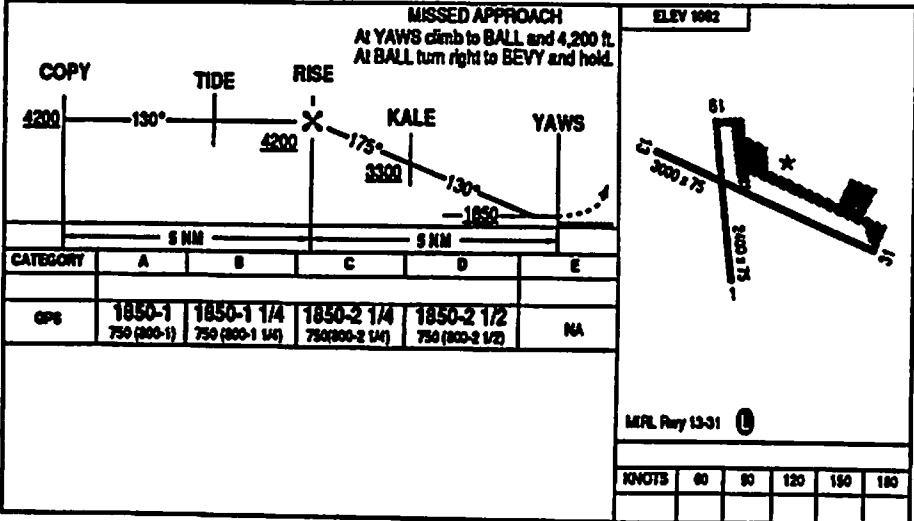
AL-2346 (FAA)

MUDGEE (MDG)
MUDGEE, VICTORIA

MUDGEE CENTER
134.3 237.8
UNCOM 122.725 (CTAF)



EXPERIMENTAL CHART
NOT FOR PUBLIC USE



GPS RWY 13

GEODEIC REF: WGS-84
42°27'N 0157°02'W

MUDGEE, VICTORIA
MUDGEE (MDG)

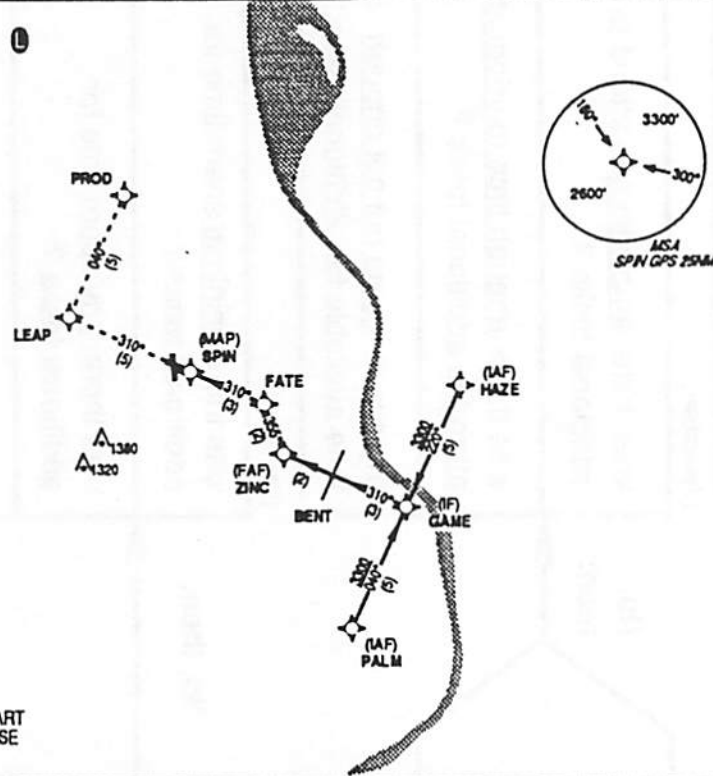
FIGURE A2-7. MUDGEE (MDG) RUNWAY 13

GPS RWY 31

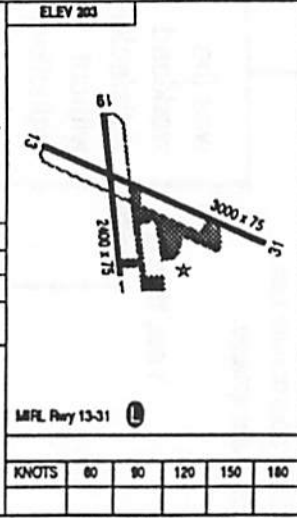
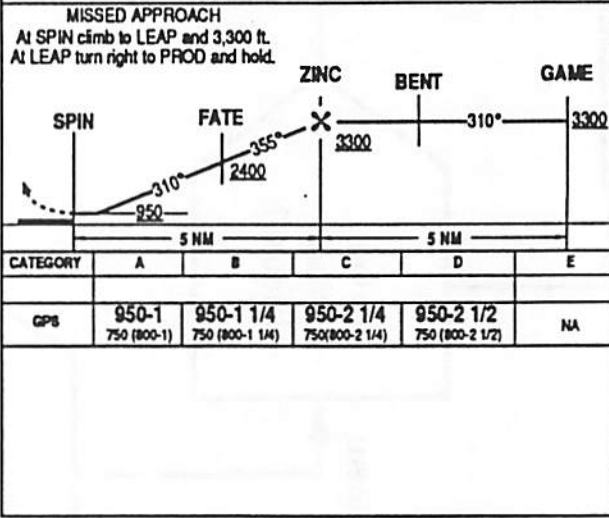
AL-31283 (FAA)

WARNAMBOOL (WMB)
WARNAMBOOL, HARMEN

WARNAMBOOL CENTER
125.15 257.3
UNICOM 123.075 (CTAF)



EXPERIMENTAL CHART
NOT FOR PUBLIC USE



GPS RWY 31

GEODEIC REF: WGS-84
42°34'N-089°42'W

WARNAMBOOL, HARMEN
WARNAMBOOL (WMB)

FIGURE A2-8. WARNAMBOOL (WMB) RUNWAY 31

MODIFIED BEDFORD PILOT WORKLOAD SCALE for instrument approach tasks

Subject rates workload on a 4 category (impossible/tolerable/satisfactory) scale and then rates spare time within category using the descriptions in the appropriate box. Use of fractions (e.g. 3.5) is acceptable.

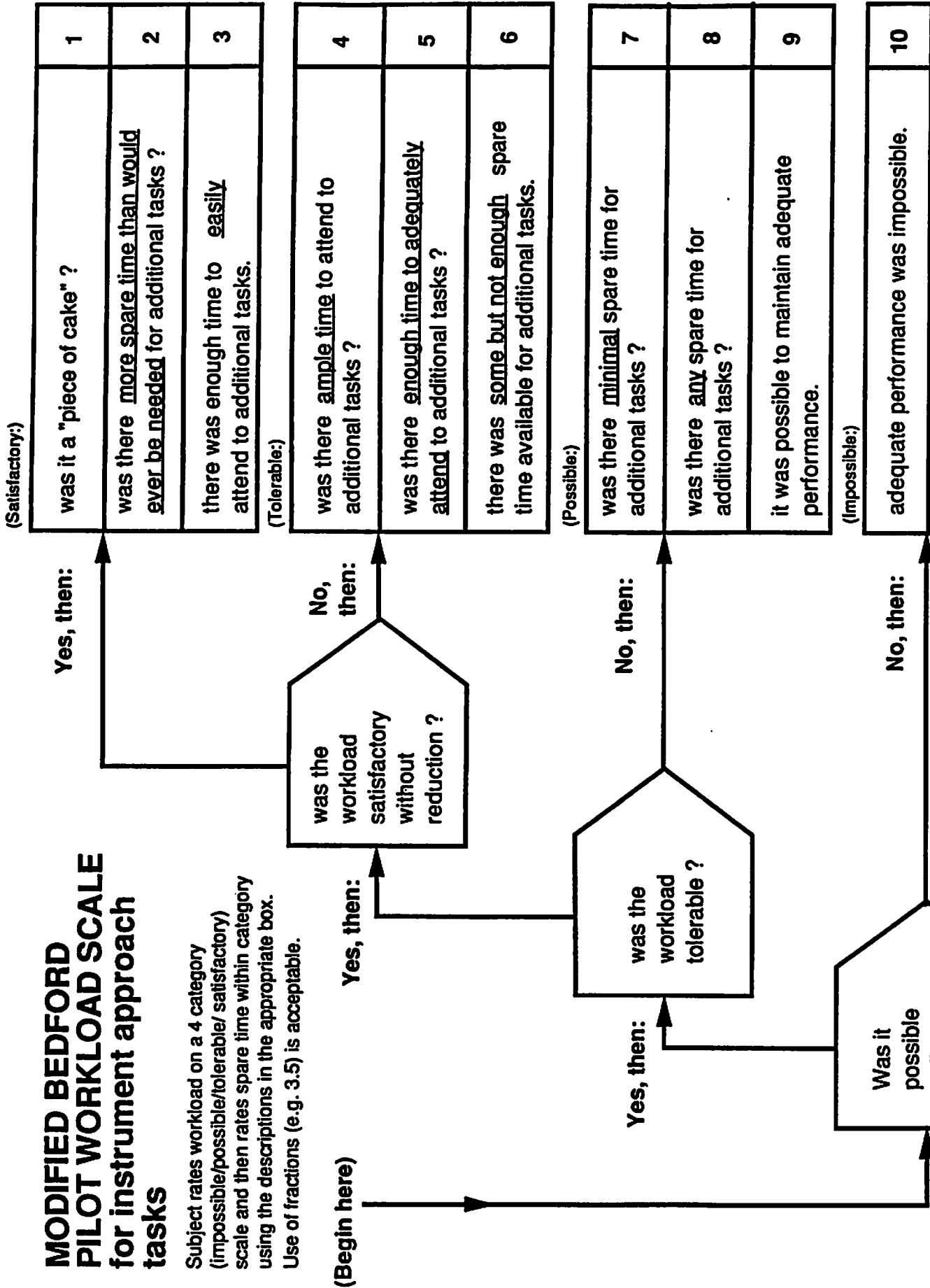


Figure A2-9. Modified Bedford Pilot Workload Scale

